

# **DRONE DESIGN AND FABRICATION BASED ON OPEN-SOURCE SOFTWARE AND HARDWARE ARCHITECTURE AIMING TOWARDS INDIGENISATION**

*A Project Report*

*submitted by*

**Lt Col K Tony Joseph  
EE19M009**

*Under the esteemed guidance of*

**Prof. Ashok Jhunjunwala**

*In partial fulfillment of the requirement for the award of the degree of*  
**MASTER OF TECHNOLOGY**



**DEPARTMENT OF ELECTRICAL ENGINEERING  
INDIAN INSTITUTE OF TECHNOLOGY MADRAS,  
CHENNAI - 600 036**

**June 2021**

## THESIS CERTIFICATE

This is to certify that the thesis titled “*Drone design and fabrication based on open-source software and hardware architecture aiming towards Indigenisation*”, submitted by **Lt Col K TONY JOSEPH (EE19M009)**, to the Indian Institute of Technology, Madras, for the award of the degree of **Master of Technology**, is a bonafide record of the research work done by him under my supervision. The contents of this thesis, in full or in parts, have not been submitted to any other Institute or University for the award of any degree or diploma.

**Prof. Ashok Jhunjunwala**

Project Guide

Department of Electrical Engineering

Indian Institute of Technology Madras

Chennai – 600 036.

Place: Chennai

Date: Jun 2021

## **ACKNOWLEDGEMENTS**

I am ever thankful to Prof. Ashok Jhunjhunwala for his vision and guidance in the conceptualization and materialization of the project. We Army officers, feel privileged and honored to have worked under his guidance. I would like to extend my sincerest gratitude to him for guiding us, and also giving us exposure to the R&D processes at IITM Research Park. I would also like to express my heartfelt gratitude to the unwavering support extended by his team at the Centre for Battery Engineering and Electric Vehicles (CBEEV) and Motorz. CBEEV was the nodal agency that facilitated the procurement of various components, extended their technical support, and provided us with an in-house designed and fabricated smart battery pack with an intelligent Battery Management System (BMS). The Motorz team worked jointly with us in the design and fabrication of the drone motor prototype. I would like to especially thank Prof. Kannan Lakshminarayan, Prof. Kaushal Jha, and Mrs. Sandhya Ravi Kumar.

I would also like to take this opportunity to thank Prof. Satyanarayanan R. Chakravarthy and his team at the EPlane company who have provided their expertise and support for drone assembly and flight tests. My deepest regards to Prof. Bhaskar Ramamurthy, Prof. David Koilpillai, and other professors at IIT Madras, who have motivated and guided us towards academic excellence.

I would like to take this opportunity to thank my organization- the Indian Army for giving me this opportunity to become a part of such a prestigious institution. I wish to thank my family for their support and encouragement during the entire period. I would like to dedicate this work to them.

Last but not the least, I would like to thank my team members in this project, Lt Col Yashvardhan Singh and Major Akhil Sharma who provided relentless support and encouragement and worked cohesively for the fruition of this project.

# ABSTRACT

Drone technology is one of the sophisticated technologies in the world. A primary objective of the project to aim towards indigenisation while building the drone. A three-pronged approach has been followed by our team subdividing the work into the flight controller, sensor programming, motor development, frame designing, and assembly. In this paper, we study frame designing and simulation analysis for a drone before assembly. After assembly test flights were conducted and flight data log analysis has been done to analyze and further optimize the drone. Firstly, CAD modeling of the frame was done and improved post iterations. Later based on the mechanical theory, a finite element model for the hexacopter is created for identifying the right material for the drone body. The linear static structural analysis under particular conditions is performed to determine the stress and deformation in the frame. The modal analysis is conducted to obtain the natural frequencies and their corresponding vibration shapes. Thus, the behavior of the system is obtained by analyzing the simulation results and the shortcomings of the structure were addressed which was beneficial for optimizing the design for the Hexacopter. Further integration of components with the frame and interfacing with the open-source Flight controller was done. Lastly, flight log analysis using Mission planner gave insight into optimizing the flight dynamics of the drone for better performance.

**Keywords:** Hexacopter, static analysis, modal analysis, flight log analysis.

# TABLE OF CONTENTS

<b>ACKNOWLEDGEMENTS</b>	<b>i</b>
<b>ABSTRACT</b>	<b>ii</b>
<b>LIST OF TABLES</b>	<b>vi</b>
<b>LIST OF FIGURES</b>	<b>vii</b>
<b>ABBREVIATIONS</b>	<b>ix</b>
<b>1 INTRODUCTION</b>	<b>1</b>
<b>2 FLIGHT DYNAMICS AND SYSTEM DESIGN</b>	<b>3</b>
2.1 Introduction . . . . .	3
2.2 Flight Dynamics . . . . .	4
2.3 Working Principle: Multirotor Drone . . . . .	5
2.4 Kinematic of a Quadcopter . . . . .	6
2.5 Block Diagram. . . . .	8
<b>3 STUDY OF DRONE FRAMES AND CAD MODELLING</b>	<b>11</b>
3.1 Introduction . . . . .	11
3.2 Multirotor Frame Configurations . . . . .	11
3.3 Study of X and V Quadcopter frames. . . . .	13
3.3.1 X-Type Frame . . . . .	13
3.3.2 V-Type Frame. . . . .	14
3.3.3 Analysis. . . . .	14
3.4 Hexacopter frame Configuration . . . . .	15
3.5 CAD Modelling of Hexacopter frame . . . . .	15
3.5.1 Basic Frame Design. . . . .	16
3.5.2 Design Iterations . . . . .	20

3.5.3	Final Design. . . . .	21
3.6	Results. . . . .	21
<b>4</b>	<b>MECHANICAL ANALYSIS OF DRONE FRAME</b>	<b>22</b>
4.1	Frame Material . . . . .	22
4.2	FEA Modelling. . . . .	23
4.3	Static Structural Analysis: CFRP vs Aluminium 6061 . . . . .	24
4.3.1	Loading and Boundary Conditions , . . . .	25
4.3.2	Von-Mises Stress Analysis. . . . .	25
4.3.3	Equivalent Strain Analysis. . . . .	26
4.3.4	Frame Deformation Analysis. . . . .	26
4.3.5	Result. . . . .	27
4.4	Modal Analysis: CFRP Frame. . . . .	27
4.4.1	Modal Analysis: Theory. . . . .	27
4.4.2	Modal Analysis using Ansys Workbench. . . . .	29
4.4.3	Inference . . . . .	31
4.5	Study of CF frame performance with varying Motor Thrust . . . . .	32
4.5.1	Motor Thrust Simulation . . . . .	32
4.5.2	Simulation Results . . . . .	33
<b>5</b>	<b>HEXACOPTER ASSEMBLY</b>	<b>34</b>
5.1	Introduction. . . . .	34
5.2	Frame Assembly. . . . .	34
5.3	Motors. . . . .	35
5.4	Electronic Speed Controllers. . . . .	36
5.5	Propellers. . . . .	36
5.6	Battery. . . . .	37
5.7	Flight Controller . . . . .	37
5.8	Companion Computer . . . . .	38
5.9	GPS Module. . . . .	39
5.10	Collision Avoidance System. . . . .	39

5.10.1 Lidar . . . . .	40
5.10.2 Millimeter wave Radar. . . . .	41
5.11 Camera with Gimbal. . . . .	41
5.12 Radio transmitter and receiver . . . . .	41
5.13 Final Prototype . . . . .	42
5.13.1 Layout. . . . .	42
5.13.2 Power supply arrangement . . . . .	42
5.13.3 Weight Calculation. . . . .	43
5.14 Flight testing. . . . .	44
5.15 Challenges faced and addressed. . . . .	46
<b>6 FLIGHT DATA ANALYSIS</b>	<b>47</b>
6.1 Introduction. . . . .	47
6.2 Mission Planner setup. . . . .	48
6.3 Flight Data Log. . . . .	48
6.4 Analysis of flight data, . . . . .	49
6.4.1 Case study 1: Position hold mode. . . . .	49
6.4.2 Case study 2: Errors/Variance . . . . .	50
6.4.3 Case study 3: Autonomous Mission. . . . .	53
6.5 Results	56
<b>7 CONCLUSION</b>	<b>57</b>

## LIST OF TABLES

3.1	X-Type Frame Specifications. . . . .	13
3.2	V-Type Frame Specifications. . . . .	14
3.3	CAD components of Hexacopter Frame. . . . .	16
4.1	Common Types of frame materials . . . . .	22
4.2	Mechanical Properties of CFRP vs Aluminium 6061. . . . .	24
4.3	Significant Vibration mode orders for CFRP frame . . . . .	30
4.4	Motor Power rating: T Motor MN4006 KV380 . . . . .	32
5.1	Motor Specifications: T Motor MN4006 KV380 . . . . .	35
5.2	Hexacopter Weight Calculations. . . . .	43
5.3	Flight Test Results of Hexacopter. . . . .	44
6.1	Comparison of Log files on Mission Planner . . . . .	49



## LIST OF FIGURES

2.1	Forces acting on a Flight . . . . .	4
2.2	Principal Axes of aerial Platform . . . . .	5
2.3	Controls of a Quadcopter. . . . .	6
2.4	Kinematic of a Quadcopter . . . . .	6
2.5	Block Diagram of a drone. . . . .	8
3.1	Common Quadcopter Configuration . . . . .	11
3.2	Multirotor Frame Configuration. . . . .	12
3.3	X-Type Frame Configuration . . . . .	13
3.4	V-Type Frame Configuration . . . . .	14
3.5	CAD Models: a) Centre Plate Assembly b ) Motor Assembly . . . .	18
3.6	CAD Model: Pipe Body frame . . . . .	18
3.7	Drone frame modelled in Fusion 360 . . . . .	19
3.8	Hexacopter Frame dimensions. . . . .	19
3.9	CAD Images of Hexacopter: a) Design 1 b) a) Design 2 . . . . .	20
3.10	Final Design: Isometric view. . . . .	21
4.1	Mesh Settings on Ansys. . . . .	23
4.2	Meshing quality and Skewness. . . . .	24
4.3	Boundary conditions for Structural Analysis . . . . .	25
4.4	Von-mises Stress analysis comparison: a) CF b) Al6061. . . . .	25
4.5	Strain analysis comparison: a) CF b) Al6061 . . . . .	26
4.6	Total Deformation analysis comparison: a) CF b) Al6061 . . . . .	26
4.7	Mode vs Natural frequency plot: Carbon Fibre Frame. . . . .	29
4.8	Participation factor: Carbon Fibre Frame . . . . .	29
4.9	CF Modal Analysis: Mode 4 and 5. . . . .	30
4.10	CF Modal Analysis: Mode 6 and 7. . . . .	31
4.11	CF Modal Analysis: Mode 9, 13, 18 and 20. . . . .	31
4.12	CF frame at 10N: a) Stress analysis b) Deformation analysis. . . . .	32
4.13	CF frame at 20N: a) Stress analysis b) Deformation analysis. . . . .	33
4.14	CF frame at 30N: a) Stress analysis b) Deformation analysis. . . . .	33

5.1	Frame Prototype assembly at NCCRD lab, IIT . . . . .	34
5.2	a) BLDC motor b) Hexacopter X configuration . . . . .	35
5.3	ESC with rating 5V 30A. . . . .	36
5.4	Foldable 1555 propeller pair- CW and CCW. . . . .	36
5.5	Six cells Lipo battery . . . . .	37
5.6	Flight Controller . . . . .	38
5.7	Companion Computer . . . . .	39
5.8	GPS Module . . . . .	39
5.9	a) RP A2 360 Lidar b) Lidar Output. . . . .	40
5.10	a) HD camera b) Gimbal 3D . . . . .	41
5.11	a) RC Transmitter b) RC receiver . . . . .	42
5.12	Assembly of Flight Controller system. . . . .	43
5.13	Final Prototype a) Front view b) Top view . . . . .	43
5.14	Test flight in progress at Chemplast cricket stadium. . . . .	45
5.15	Ground Control Station setup. . . . .	45
6.1	Basic Mission Planner GUI. . . . .	47
6.2	Mission Planner: a) Firmware selection b) Drone Calibration . . . . .	48
6.3	Hexacopter in Position Hold mode . . . . .	49
6.4	Flight Trajectory on Matlab . . . . .	49
6.5	Manual Flight parameters: Altitude and GPS . . . . .	50
6.6	Manual Flight parameters: Vibration along X Y Z axes . . . . .	50
6.7	Manual Flight parameters: Attitude Performance . . . . .	51
6.8	Flight parameters: Yaw Variance . . . . .	51
6.9	Flight parameters: Throttle Output error . . . . .	52
6.10	Hexacopter Autonomous mission. . . . .	53
6.11	Auto Flight Trajectory on Matlab . . . . .	53
6.12	Auto Flight parameters: Altitude and GPS . . . . .	54
6.13	Auto Flight parameters: Vibration along X Y Z axes . . . . .	54
6.14	Auto Flight parameters: Voltage and load . . . . .	55
6.15	Auto Flight parameters: Roll movement . . . . .	55
6.16	Auto Flight parameters: Pitch movement . . . . .	56

# ABBREVIATIONS

<b>AHRS</b>	Attitude and Heading Reference System
<b>AI</b>	Artificial Intelligence
<b>Al</b>	Aluminium
<b>BLDC</b>	Brushless DC
<b>CAD</b>	Computer-Aided Design
<b>CFRP</b>	Carbon Fibre Reinforced Polymer
<b>CG</b>	Centre of Gravity
<b>CW</b>	Clockwise
<b>CCW</b>	Counter Clockwise
<b>EKF</b>	Extended Kalman Filter
<b>ESC</b>	Electronic Speed Control
<b>FEA</b>	Finite Element Analysis
<b>FMCW</b>	Frequency Modulated Continuous Wave
<b>GCS</b>	Ground Controller Station
<b>GPS</b>	Global Positioning System
<b>HUD</b>	Head-Up Display
<b>I2C</b>	Inter-Integrated Circuit
<b>IMU</b>	Inertial Measurement Unit
<b>LiPo</b>	Lithium Polymer
<b>MAVLink</b>	Micro Air Vehicle Link

<b>PID</b>	Proportional–Integral–Derivative
<b>PWM</b>	Pulse Width Modulation
<b>RC</b>	Remote Control
<b>RPM</b>	Revolutions Per Minute
<b>RTL</b>	Return to Launch
<b>UAV</b>	Unmanned Aerial Vehicle
<b>VTOL</b>	Vertical Take-off and Landing
<b>WP</b>	Way Point
<b>3-D</b>	Three Dimensions
<b>6-DOF</b>	Six-Degrees of Freedom

# CHAPTER 1

## Introduction

### Motivation

Drone technology is one of the most promising technologies of the present era. Today Unmanned Aerial Vehicles (UAVs) have caught human imagination because of their innovative applications in the field of defense, logistics, disaster management, search and rescue, firefighting, surveillance, monitoring, agriculture, aerial photography etc. With their agility and ability to reach inaccessible places, drones are a force multiplier in any operation. Countries across the world have realized the potential of drones and are investing in the growth of innovation in this field.

Though the Indian defence forces and industry have already started harnessing this technology we are still at a nascent stage with respect to India's UAV program-indigenous development of UAVs in India. We are still primarily dependent on imported hardware and software. **We need to have complete control of drone technology right from airframe to autopilot, from the battery to motors, from the control station to communication systems** to leverage the technology and be able to customize the system as per user requirement. Only then we can handle the technology with trust, confidence, and no sabotage risks.

This project attempts to design and develop frame structure, motors, and battery in-house and further utilize open-source autopilot software for building drones. The project team involved three Army officers working under Prof Ashok Jhunjunwala. The project was extended technical support from the Centre for Battery Engineering and Electric Vehicles (CBEEV) and Motorz startup at IITM Research Park under Professor's guidance. CBEEV was the nodal agency that facilitated the procurement of various components, extended their technical support, and provided us with an in-house designed and fabricated smart battery pack with an intelligent Battery Management System (BMS) under the guidance of Prof Kaushal Jha. For motor design and manufacturing, technical expertise was extended by Motorz, a startup under the

guidance of Prof Kannan Lakshminarayan at Telecom Centre for Excellence (TCOE). In addition, support for frame fabrication, assembly, and professional drone pilot assistance was provided by the e-plane company, a drone startup under the guidance of Prof. Satyanarayanan R. Chakravarthy of the Aerospace department.

The scope of work for our project team involved the following:

- Frame design, optimization, and assembly.
- Sensor integration along with 4G communication support.
- Flight Controller and companion computer integration
- Flight testing and post-mission flight log analysis.
- Design and fabrication of BLDC motors for drones
- Live Object detection using AI application at GCS
- Smart battery Interface development and testing/ trials

The present thesis covers the designing/fabrication of a hexacopter frame, drone assembly, and optimization aspects and also covers the flight data log analysis for the drone. The hexacopter is intended to be used as a payload-type drone for camera/cargo payload.

### **Thesis Objectives:**

- To study UAV flight aerodynamics and design.
- Study various frame configurations and model Hexacopter frame using CAD.
- Identification of suitable frame material and carrying out structural and total deformation analysis on Hexacopter frame in ANSYS software.
- Hexacopter assembly and integration of components.
- Carry out Post-flight analysis of Hexacopter and optimize the design.

# CHAPTER 2

## FLIGHT DYNAMICS AND SYSTEM DESIGN

### 2.1 Introduction

UAVs or drones are remotely piloted or autonomously controlled aerial platforms. There are primarily three types of UAVs: fixed-wing drones, multi-rotor drones, and hybrid drones.

#### **Fixed-Wing UAVs**

Fixed-wing drones are winged pilotless aircraft that have actuators like ailerons, elevators, and rudder similar to a small airplane. They are designed to cover longer distances and carry a heavier payload. The major drawback is that they require a launch mechanism and runway for landing as they don't have Vertical Take-off and Landing (VTOL) capability.

#### **Multi-copter/Multi-rotor**

Multicopters are those aircraft that are lifted and propelled by multiple horizontal rotors. Multi-rotor drones are mostly used for short-duration flights and cover shorter distances. They consume more energy since they can't glide like fixed-wing UAVs. Types of multi-copters are:

- Quadcopter. It has four horizontal rotors- two spinning clockwise (CW) and the other two spinning counter-clockwise (CCW). Its main characteristic is its high maneuverability.
- Hexacopter. It has six rotors. It is more stable than the quadcopter due to its higher number of rotors. Also, it can operate with one motor failure.
- Octocopter. It has eight rotors. This is the most stable multi-copter of the three analyzed categories, being able to carry a relatively larger payload. An increase in the number of motors increases the design cost and complexity.

## Hybrid drones

A hybrid drone is a newer concept vis-à-vis the other UAV platforms. They are hybrid in the sense that they are equipped with both wings and rotors which allow for VTOL (like the multi-rotor drone) as well horizontal flight like fixed-wing drones. This makes it possible to cover longer distances and carry a heavier payload than other drones.

## 2.2 Flight Dynamics

Before understanding the flight dynamics of a drone, it is essential to understand the basics of aerodynamics. At any given point in time, four forces act on a flight:

- **WEIGHT**, which acts downwards in the direction of gravity and brings the flight downwards.  $\text{Weight} = \text{mass} \times \text{gravity}$
- **LIFT**, which acts upwards opposite to weight and lifts the flight upwards.
- **THRUST**, produced by the propellers gives forward motion to the flight.
- **DRAG**, which acts opposite to resist thrust. The forward motion of the aircraft is opposed by the drag force, which is produced by the viscosity of air. This drag force is overcome by the thrust force.

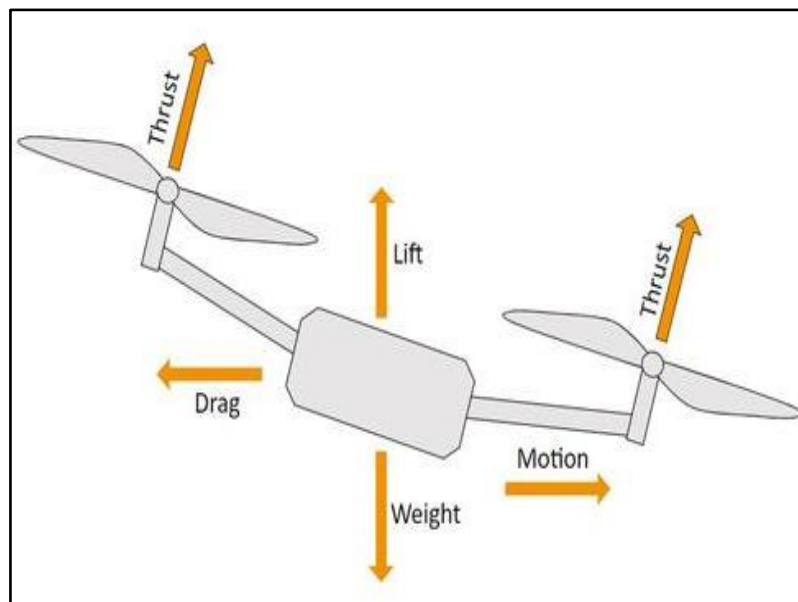


Figure 2.1: Forces acting on a flight. (rcbenchmark.com)

The movement of an aircraft is controlled by rotating it along three mutually perpendicular axes. These axes are:



- Longitudinal axis (front-back direction). The aircraft performs **Roll** movement along this axis.
- Lateral axis (left-right direction). The aircraft performs **Pitch** movement along this axis.
- Perpendicular axis (top-bottom direction). The aircraft performs **Yaw** movement along this axis.

A combination of movement along these three mutually perpendicular axes results in the overall movement of the aircraft.

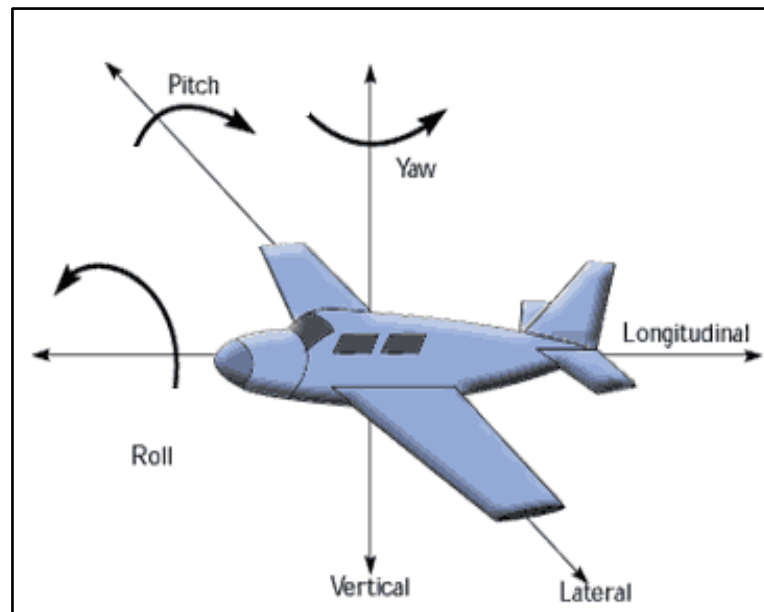


Figure 2.2: Principal axes of aerial platform. (novatel.com)

## 2.3 Working Principle: Multirotor Drone

For a conventional fixed-wing aircraft, its roll, pitch, and yaw movements are controlled using control surfaces i.e ailerons, elevators, rudder. But the movements of a drone are controlled by varying the relative thrusts of each of the rotors, i.e controlling the angular speed of the propellers. Each propeller produces a thrust individually by pushing the air downwards. But the important fact is that adjacent motors rotate in opposite directions: one in the clockwise direction and the other in the anti-clockwise direction. This ensures that the overall torque is zero so that the drone doesn't spin.

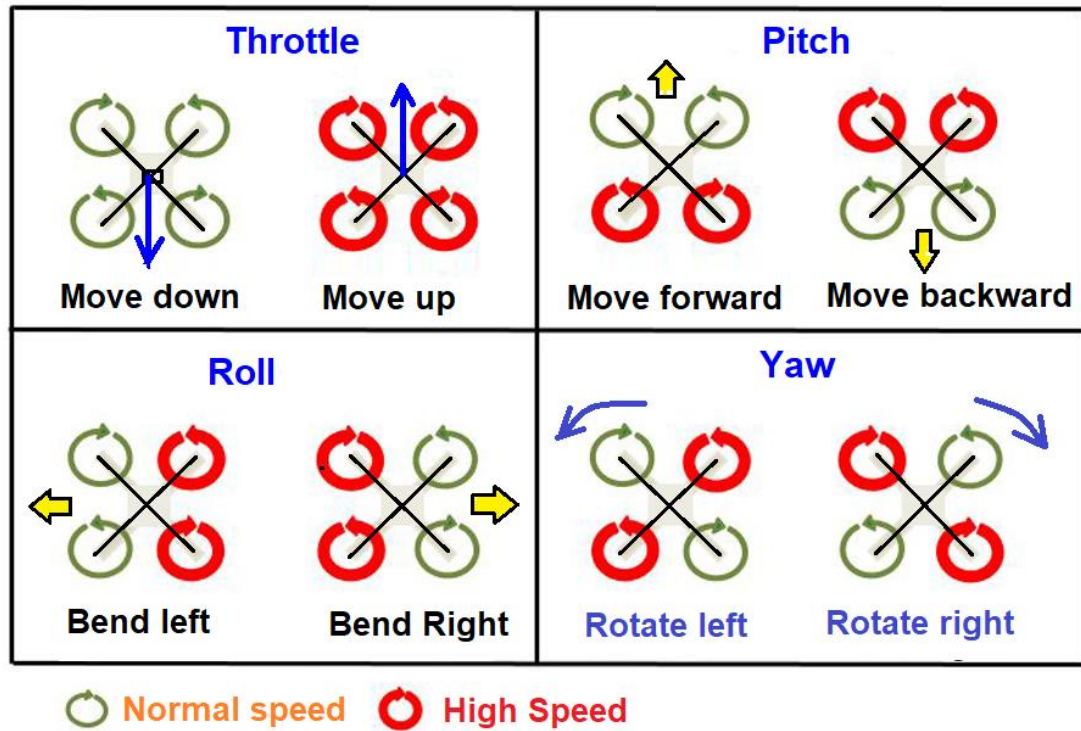


Figure 2.3: Controls of a Quadcopter. (cfdflowengineering.com)

## 2.4 Kinematic of a Quadcopter

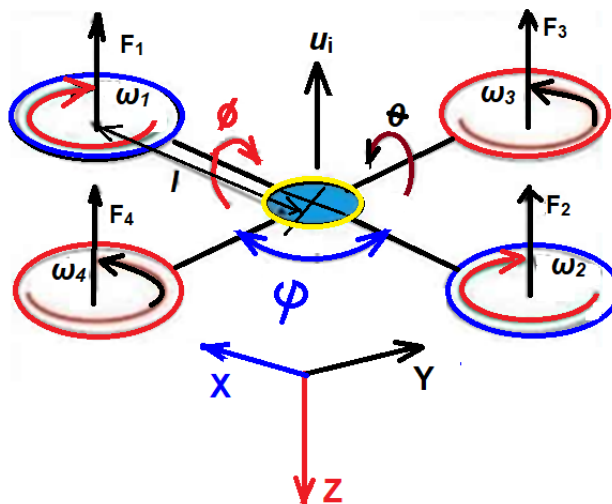


Figure 2.4. Kinematic of a Quadcopter. (cfdflowengineering.com)

The thrust produced by each propeller is perpendicular to the plane of rotation of propellers. It is directly proportional to the square of the angular velocity of the propeller.

$$F_i = k_f \times \omega_i^2$$

If  $L$  is defined as the distance between two motors or propellers for any diagonal of drone, then the reaction moments about the X-axis and Y-axis

$$M_x = (F_3 - F_4) \times L$$

$$M_y = (F_1 - F_2) \times L$$

### **Newton's second law of motion**

For linear motion: Force = mass  $\times$  linear acceleration

For rotational motion: Torque = inertia  $\times$  angular acceleration

#### **a) Hovering Motion**

- **Equilibrium Conditions for hovering**

$$mg = F_{eq} \text{ where } F_{eq} = F_1 + F_2 + F_3 + F_4$$

$$\text{All moments} = 0$$

- **Equation of motion**

$$m = F_{eq} - mg$$

$$m = 0$$

#### **b) Ascent or Descent (Throttle up/down)**

- **Conditions for hovering (rise)**

$$mg < F_{eq}$$

$$\text{All moments} = 0$$

- **Conditions for Fall**

$$mg > F_{eq}$$

$$\text{All moments} = 0$$

- **Equation of motion**

$$m = F_{eq} - mg$$

$$m > 0$$

#### **c) Yaw Motion**

- **Conditions for hovering**

$$mg = F_{eq}$$

$$\text{All moments} \neq 0$$

- **Equation of motion**

$$mass * linear\ acceleration = F_{eq} - mg$$

$$I_{zz} * angular\ acceleration @\ Z\text{-axis} = M1 + M2 + M3 + M4$$

#### d) Pitch and Roll Motion

- **Conditions for hovering**

$$mg < F_{eq}$$

$$All\ moments \neq 0$$

- **Equation of motion**

$$mass * linear\ acceleration = F_{eq} - mg$$

$$I_{xx} * angular\ acceleration @\ x\text{-axis} = (F3 - F4) \times L$$

## 2.5 Block Diagram

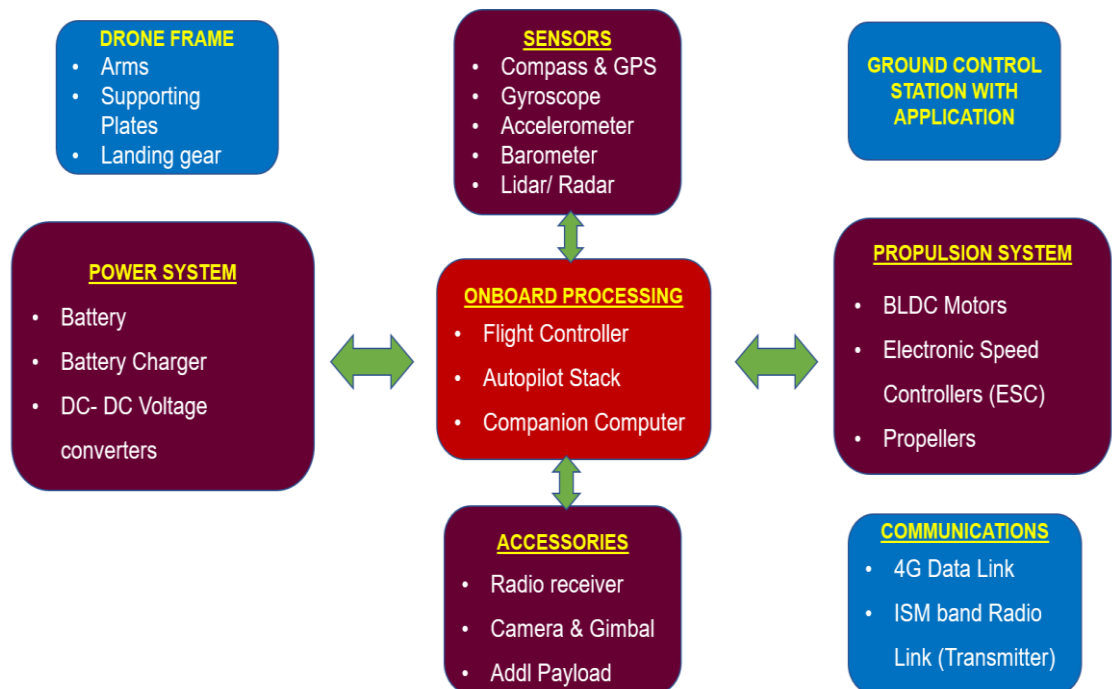


Figure 2.5: Block Diagram of a Drone

The major components of a drone are listed as under:

**a) Frame:**

- It should have sufficient strength to hold the propeller momentum and additional weight of motors, camera, and payload.
- Sturdy and less aerodynamic resistance.

**b) Propellers:**

- The speed and load lifting ability of drone depends on shape, size, and number of propellers
- The long propellers create huge thrust to carry heavy loads at a low speed (RPM) and less sensitive to change the speed of rotation
- Short propellers carry fewer loads. They change rotation speeds quickly and require a high speed for more thrust.

**c) Motor**

- Both motors brushless and brushed type can be used for drones
- A brushed motor is less expensive and useful for small-sized drones
- Brushless-type motors are comparatively more powerful and energy-efficient. But motor speed regulation is done using the Electronic Speed Controller (ESC).

**d) ESC (Electronic Speed Controller)**

- ESC is used to connect the battery to the electric motor for the power supply
- It converts the PWM signal from the flight controller to the revolution per minute (RPM) of the motor. Each ESC controls a particular motor of the drone.

**e) Flight Controller (FC)**

- It is the computer processor which manages balance and telecommunication controls using different transmitter
- Sensors are located in this unit for accelerometer, barometer, magnetometer, gyro, compass, and GPS
- Collision avoidance systems like Lidar, Radar can also be integrated as part of the system.

**f) Radio Transmitter**

- sends the radio signal to ESC to pilot to control motor speed.

**g) Radio Receiver:**

- Received the signal from the pilot. This device is attached to the drone.

**h) Battery**

- Lithium Polymer (LiPo) is used mostly for drones due to its high capacity and high discharge rate.
- For quadcopter, the battery can have 3 cells (3S) or 4 cells (4S) whereas Hexacopter requires 6 cells (6 S), each cell being 3.7 V(nominal).

## CHAPTER 3

# STUDY OF DRONE FRAMES AND MODELLING USING COMPUTER-AIDED DESIGN

### 3.1 Introduction

A drone frame is generally the first thing decided before assembling other components and sensors. It is chosen based on the application it is to be used- racing, cargo payload, photography etc. Drone frame modelling is useful to analyse the reliability of the frame and to determine the type of rotor and propeller in order to ensure the necessary flight acceleration. The frame has to be designed to be as light as possible, meanwhile maintaining the strength to carry the load. Our study focuses on designing a sturdy frame for a drone with a payload mission.

### 3.2 Multirotor Frame Configurations

The shape of the frame is dictated by the layout of its arms. We will focus on the mainstream 4 and 6 arm setups. For a quadcopter, there are many options like Plus, True-X, Stretched X, H frames or V-tails etc.

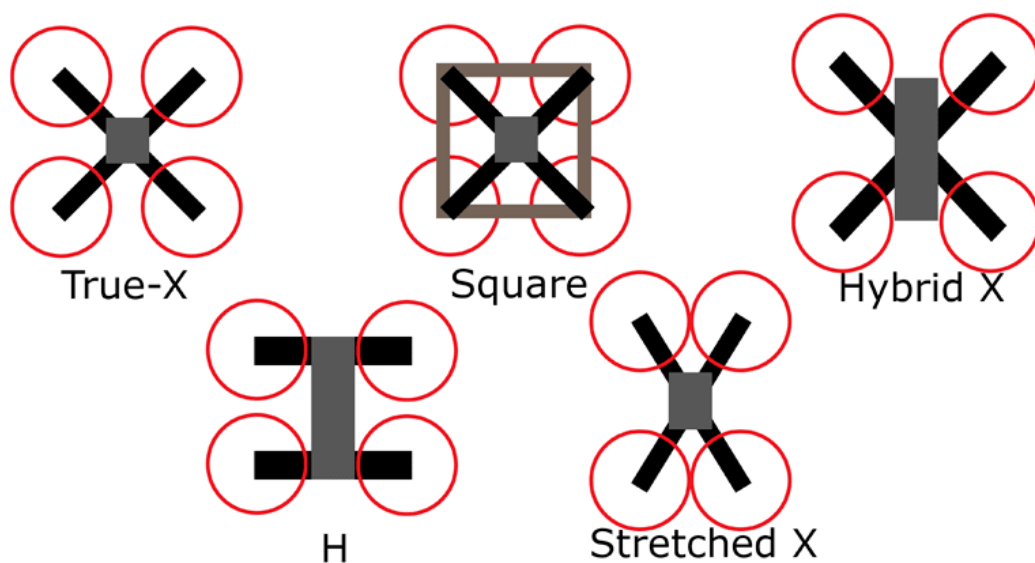


Figure 3.1: Common Quadcopter configuration. (dronenodes.com)

We shall be focussing on the most widely used frame configurations which are true for multicopter. They are mainly the Plus and X configurations.

- **X Configuration.** The true X configuration is shaped akin to X shape geometry with which a motor is mounted to each end of the arms. The direction of drone movement is along a perpendicular bisector between two arms of the frame. The perpendicular distance between the centre of each motor is equal, therefore giving the quadcopter the same level of stability on all axis.
- **Plus (+) Configuration.** A plus frame is similar to an X frame except that the frame orientation is rotated by  $45^\circ$ . The direction of drone movement is along one of the arms of the frame. A plus frame has the advantage that each motor is responsible for rotational movement in only one axis, theoretically allowing finer control of the drone. However, plus frames are more prone to breakage with a single arm taking all the impact.

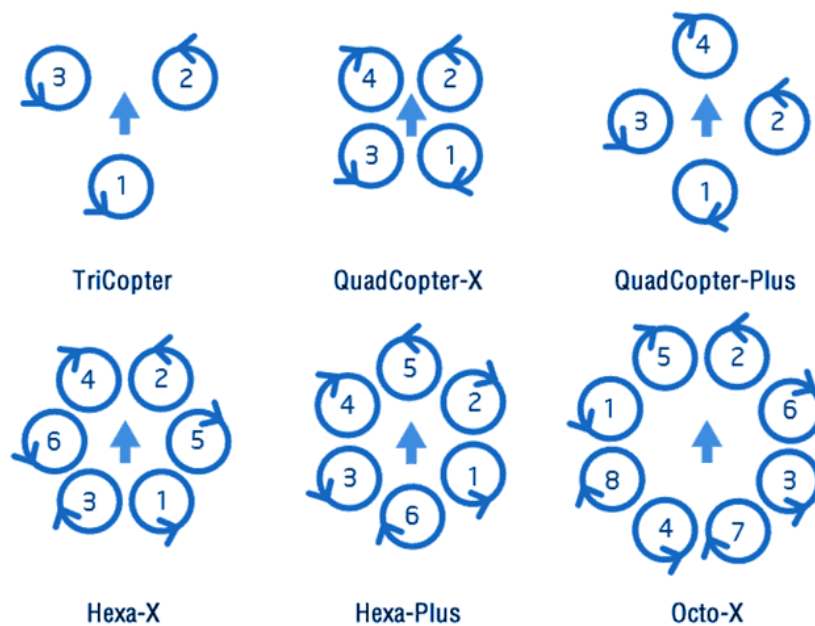


Figure 3.2: Multicopter configuration. (droneomega.com)



### 3.3 Study of X and V Quadcopter frames

Before starting work on designing a Hexacopter frame at the lab, an initial study was done using prefabricated frames procured for gaining confidence in the assembly of drones. This was also from a safety perspective to avoid dangers to man or material when conducting trials of the open-source autopilot software on a custom flight controller board. Following quadcopter models were assembled and studied:

#### 3.3.1 X-type frame

The specifications of our X-type frame procured are as under

Table 3.1: X type frame Specifications

<b>Model</b>	Q450
<b>Material</b>	Glass Fiber + Polyamide Nylon
<b>Wheelbase (mm)</b>	450
<b>Weight (gm)</b>	330 (Q450 Frame)
<b>Arm Size (L x W) mm</b>	220 x 40
<b>Landing Gear Material</b>	ABS Plastic
<b>Landing Gear Weight (gm)</b>	75
<b>Battery</b>	4S
<b>Propeller</b>	Size 1045 (Dia-10 inch Pitch 4.5 inch)



Figure 3.3: X Type frame configuration

### 3.3.2 V-Type frame

The specifications of our V type frame procured are as under:

Table 3.2: V-type frame Specifications

<b>Model</b>	TBS 500
<b>Material</b>	Carbon Fiber + Polyamide Nylon
<b>Wheelbase (mm)</b>	500
<b>Weight (gm)</b>	400
<b>Arm Size (L x W) mm</b>	220 x 40
<b>Battery</b>	3S
<b>Propeller</b>	Size 8045 (Dia-8 inch Pitch 4.5 inch)



Figure 3.4: V-Type frame configuration

### 3.3.3 Analysis

Post assembly of the components, the gross weight of the X-type frame quadcopter was 1.3 kg whereas for the V frame quadcopter it was 1.8 Kg with companion computer mounted. It was observed that both frames had their advantages. The V-type frame had more space for accommodating camera and sensors compared to an X-type frame. But the X-type frame was found to be more stable and efficient, being symmetrical. Also based on flight trials carried out on both these platforms, the X-type was more stable during flight.

### **3.4 Hexacopter Frame Configuration**

The model of the hexacopter is symmetrical like a hexagon, with the center of gravity (CG) of the hexacopter coinciding with the center of the hexagon. A hexacopter utilises its six motors to drive/rotate its propellers. Of the six propellers, three propellers spin in one direction while the other three spin in the opposite direction so that the net torque is zero. The rotation of these propellers produces the necessary thrust to give the lifting movement to the entire frame. Now the Hexacopter frame configuration is generally recognized as two types: the Plus (+) and X configurations.

### **3.5 CAD Modelling of the Hexacopter frame**

Based on usage, the size of the hexacopter was finalized to be a sub 10 kg weight model. Before building the actual model, 3D modelling and material selection is essential to understand and optimise the design of the model.

In its implementation, Hexacopter was to be built physically, thus every detail of the body frame is very important. While designing the body frame of Hexacopter, it is important to know the total weight of the Hexacopter which includes the weight of the frame, electronic components, motors, propellers, and sensors. Thus, Frame Material selection is important while designing the frame to keep it lightweight and durable.

#### **Objective**

- To design simple and multi-functional frame for adequate payload capacity
- Sturdy and spacious enough to add accessories
- Simple yet aesthetically appealing design
- Should be cost-effective
- Easy to assemble and dismantle
- Scalability



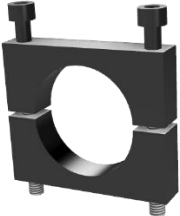
### 3.5.1 Basic Frame design


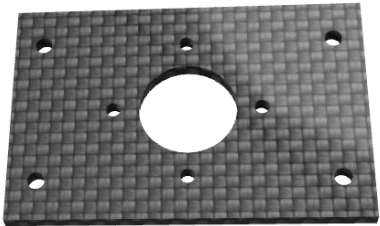
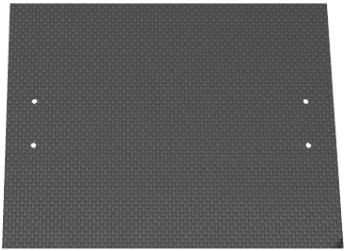

The modelling of the frame is carried in Autodesk Fusion 360 software, taking into consideration the safety requirements, smooth functioning, and optimum utilization of propellers, motors, and electrical equipment. For this model, the size of the frame is decided first followed by the selection of the suitable size of motors and propellers.

#### Design Steps

Basic components of the frame designed to scale in CAD software along with their dimensions are listed as under:

Table 3.3: CAD Components of frame

Component	Image
<b>Pipe</b> Outer Diameter 20mm Thickness 1mm	
<b>T Joint</b> Inner Diameter 20mm	
<b>Single Pipe Clamp</b> Inner Diameter 20mm	

<p><b>Two Pipe Clamp</b> Inner Diameter 20mm</p>	
<p><b>Motor Plate</b> Dimensions- 40x60x2 mm Centre hole Diameter- 16.5mm Motor mount Hole Diameter- 2.5 mm Corner Hole Diameter- 3mm</p>	
<p><b>FC Plate</b> Dimensions- 186x145x1 mm <b>Battery Plate</b> Dimensions- 198x78x1mm</p>	
<p><b>FC Enclosure</b> Dimensions- 185x150x100 mm Thickness – 1mm</p>	

### Assembly of Frame Parts

The basic components have been further assembled to form the pipe body frame, centre plate assembly, and motor assembly.



Figure 3.5: CAD Models a) Centre plate assembly b) Motor assembly



Figure 3.6: CAD Model: Pipe body frame

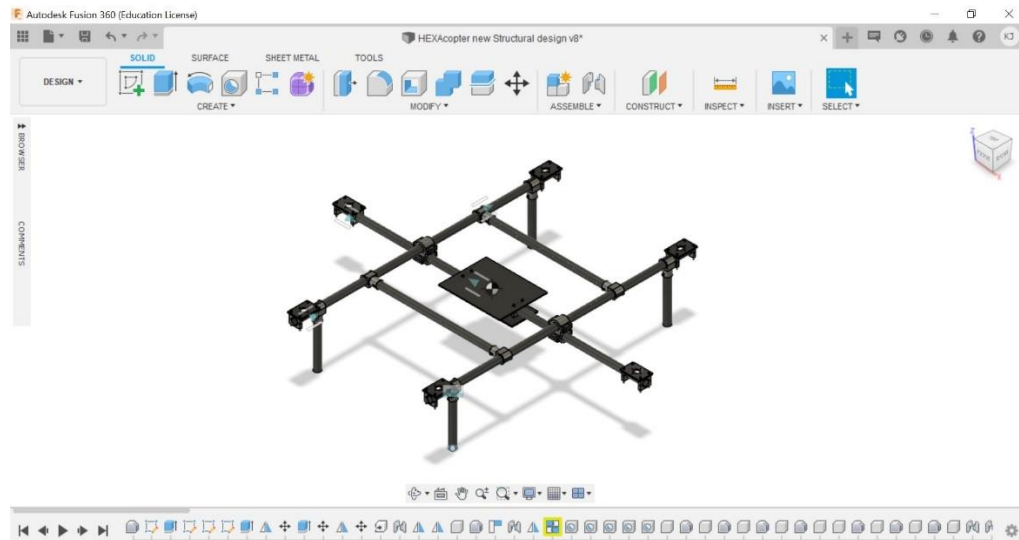


Figure 3.7: Drone frame modelled in Fusion360

### Dimensions of Frame

The dimensions of the basic Hexacopter frame are given in the Figure below:

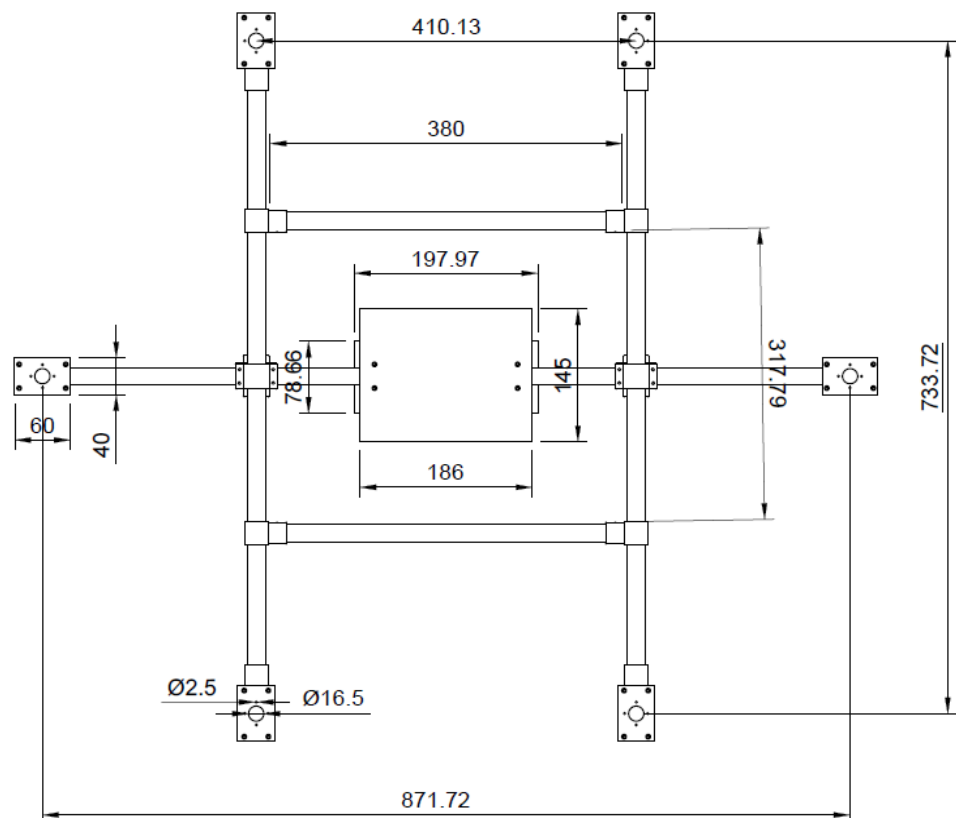


Figure 3.8: Hexacopter frame dimensions

### 3.5.2 Design Iterations

Designing needs to be done by trial and error and has to be incrementally improved. Following the same approach, the design was improved after some iterations. Three major iterations were carried out before finally achieving the desired performance from the drone.

#### Design 1.

Design 1 consisted of the Flight controller enclosure and the battery housed on the Central arm of the drone. Due to the current layout, the frame configuration chosen was Plus (+). Though stable, the centre of gravity was not exactly at the frame centre. Additionally, there was an issue of lack of space for wiring, in and out of the enclosure.

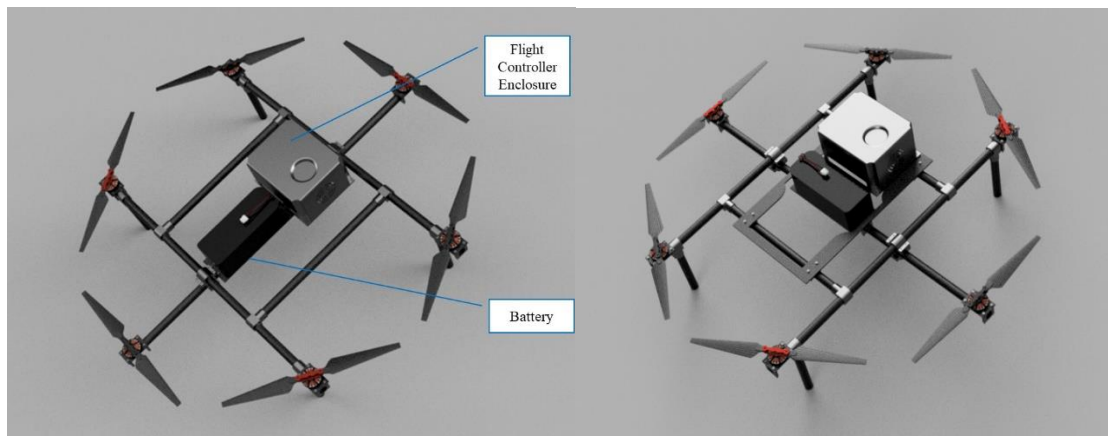


Figure 3.9: CAD Images of Hexacopter: a) Design 1 b) Design 2

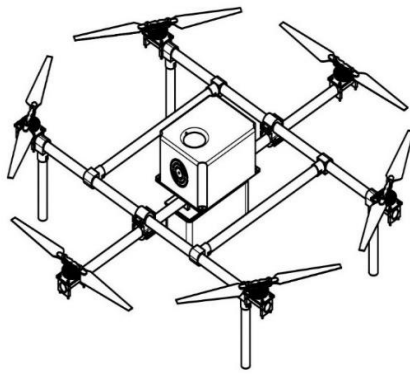
#### Design 2.

Continuing with the Plus (+) frame configuration, the battery was realigned to the frame centre whereas the Flight controller enclosure was shifted to the lateral support arm. An additional carbon fibre sheet was fixed to support the enclosure. Though the frame stability increased but this resulted in excess frame weight thereby reducing payload capacity.



### 3.5.3 Final Design

Based on the inferences drawn from the previous two designs, the frame was redesigned to accommodate both the battery and Flight controller enclosure at the Frame centre. The battery plate was shifted beneath the flight controller plate. The frame was reconfigured for 'X' geometry which provided more room space for mounting of additional components in the Hexacopter. Also, the additional plate fixed was removed, thereby reducing frame weight.



**Figure 1**Figure 3.10: Final Design: Isometric view

## 3.6 Results

In this research, both Plus (+) and X configuration were studied for frame design as it provided that flexibility to build the drone as per the requirement. Though initial design trials were done with Plus configuration but researching on the topic, the final design was configured as X configuration. A hands-on experience was obtained while assembling and configuring the X and V type quadcopters initially. This was useful towards building the larger hexacopter frame and its assembly.

## CHAPTER 4

### MECHANICAL ANALYSIS OF DRONE FRAME

#### 4.1 Frame Material

A frame is a structure that houses all the components including motors, sensors etc in a drone. Hence the frame has to be sturdy yet light to ensure all components are in place during all flight maneuvers. The common type of materials used in a frame are Balsa wood, carbon fibre, Aluminium alloys, PLA/ABS and composites.

Table 4.1: Common Type of Frame materials

Material	Advantages	Disadvantages	Cost Factor
Balsa wood	Lightweight Easy to work	Low strength	Low
PLA/ABS	3D printing feasible	3D printer required	Mid
Aluminium	Strong and Lightweight	Machining skills required	High
Carbon Fibre	Very Tough and lightweight	Signal interference	Very High

Based on the comparative analysis, carbon fibre, and aluminum alloy are the preferred choices for designing the Hexacopter frame. The suitable material for the Hexacopter frame can be selected by carrying out the Finite Element Analysis (FEA) of the structure for these two shortlisted materials –

- **Aluminium 6061 alloy**
- **Epoxy Carbon UD (230 GPa) or Carbon Fibre Reinforced Polymer (CFRP).**

## 4.2 FEA Modelling

Finite Element Analysis (FEA) based on finite Element Method (FEM) is a method of mathematically modeling and solving the stresses on an engineering design. It enables us to optimize and validate the product design and further investigate the design shortcomings. Load conditions, boundary conditions, and material models are defined in ANSYS software. Based on these conditions, a computer-assisted simulation is performed and analyzed.

### Meshing

Meshing is one of the most important steps in performing an accurate simulation using FEA. A mesh is made up of elements that contain nodes (coordinate locations in space that can vary by element type) that represent the shape of the geometry. Meshing is the process of converting irregular shapes into more recognizable volumes called “elements.”

### Mesh Settings.

In this study, the 3D CAD model of hexacopter was transferred into ANSYS software to prepare the finite element model. Meshing was performed by using a Tetrahedral element meshing type for FEA as shown in Figure. The FEA model has 612556 nodes and 330074 elements. Element size was chosen to be 5 mm. The Figure below shows the drone frame post meshing:

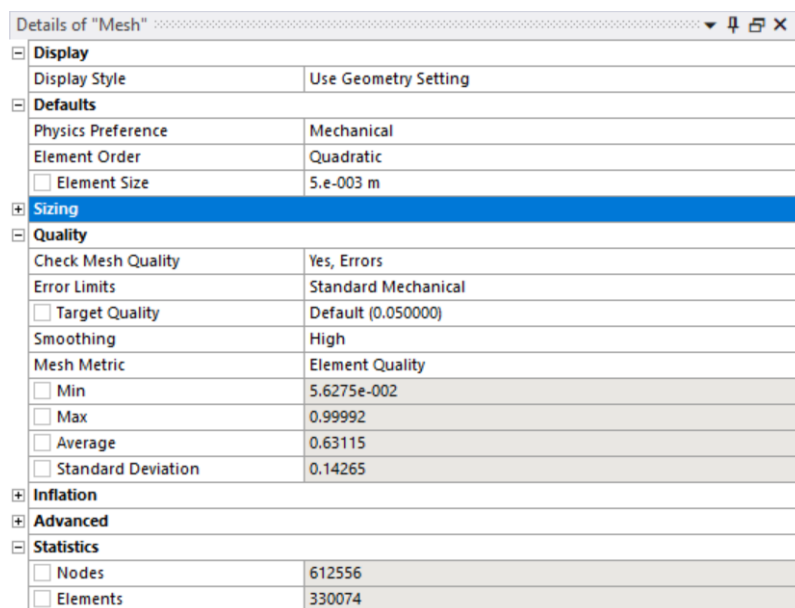


Figure 4.1: Mesh Settings on Ansys

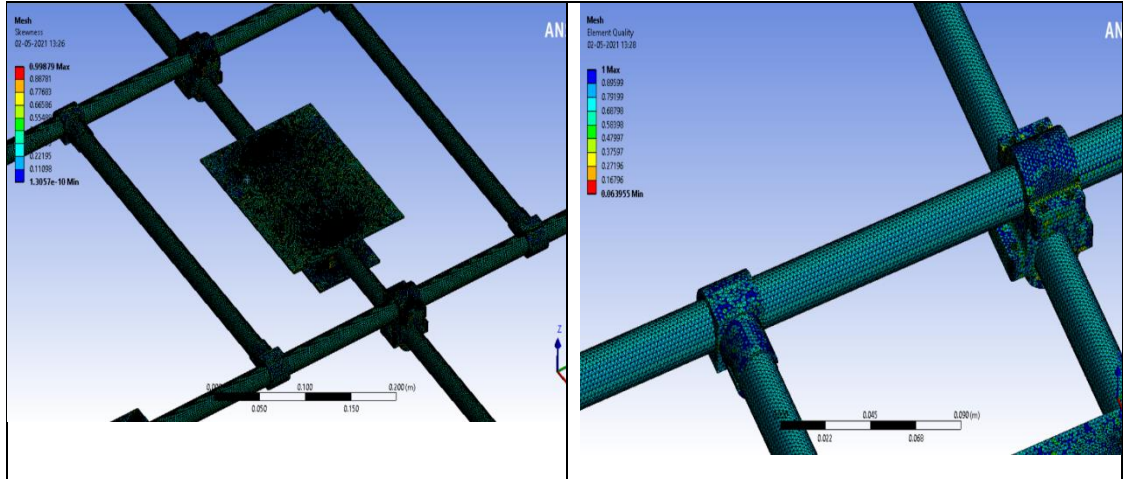


Figure 4.2: Meshing Quality and Skewness

### 4.3 Static Structural Analysis: CFRP vs Aluminium 6061

**Static structural analysis** is one of the most common types of structural analysis using the Finite Element Method. It determines the displacements, stresses, strains, and forces in **structures** or components caused by various loads. These simulations enable us to avoid design failures.

For a drone, its frame is the main weight-bearing component which i.e subjected to high tensile and compressive loads. So, we shall be comparing the hexacopter frame by assigning and comparing two different materials on Ansys Workbench – CFRP and Aluminium 6061. A comparison of their mechanical properties in Ansys is as under:

Table 4.2: Mechanical Properties of CFRP vs Aluminium 6061

Parameter	Epoxy Carbon UD (230 GPa)	Aluminium 6061 alloy
Density	1518 kg/m <sup>3</sup>	2703 kg/m <sup>3</sup>
Young's Modulus	7.78 GPa	68.9 GPa
Initial Yield Strength	290 MPa	290 MPa
Poisson's Ratio	0.27	0.33

### 4.3.1 Loading and Boundary Conditions

Structural analysis is carried out on the base plate of Hexacopter in ANSYS software. the Hexacopter body is considered as the load and the base is fixed. Various conditions for stress, strain, and deformation are checked when the applied motor thrust is maximum ie at 20 N. Meshing resolution used is fine to get accurate results.

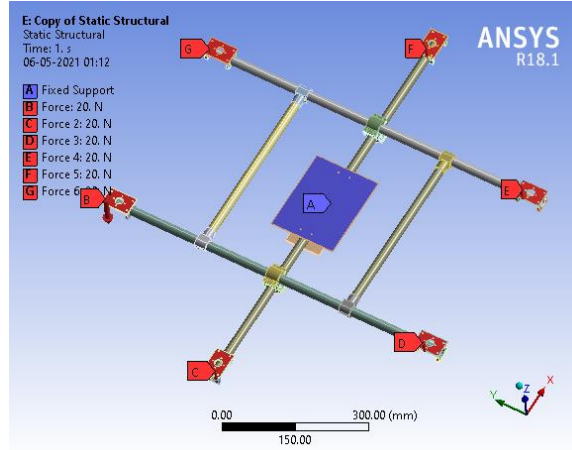


Figure 4.3: Boundary Conditions for Structural analysis

### 4.3.2 Von-mises stress analysis

When the applied thrust is 20 N, it is observed that the equivalent stress for carbon fibre material is **51.94 MPa** whereas, for Aluminium 6061, the equivalent stress is **83.2 MPa**. Thus, the performance of the carbon fibre frame is better compared to the Aluminum frame though both the materials are within their respective safety limits.

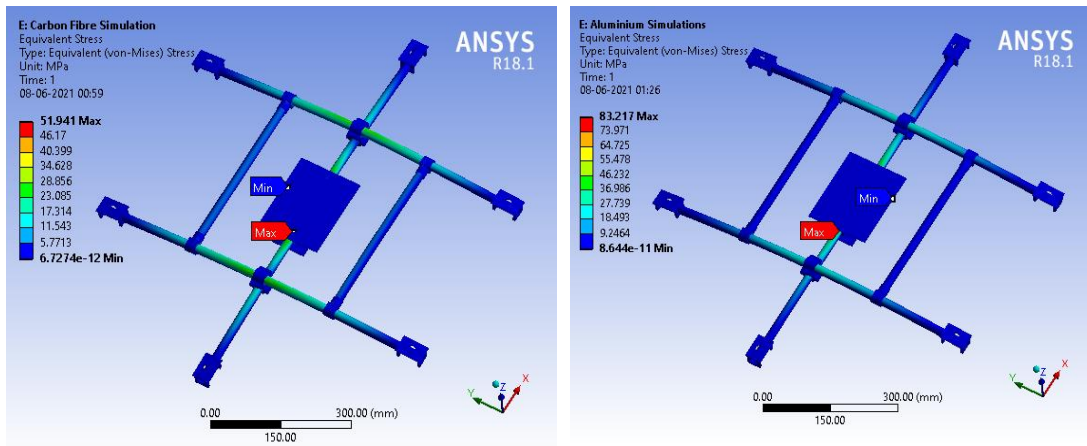


Figure 4.4: Von-mises Stress Analysis Comparison: a) Carbon fibre b) Al 6061

### 4.3.3 Equivalent Strain analysis

When the applied thrust is 20 N, it is observed that the equivalent strain on carbon fibre material is **0.000794mm** whereas, for Aluminium 6061, the equivalent strain is **0.00578mm**. Thus, the performance of the carbon fibre frame is better compared to Aluminum alloy.

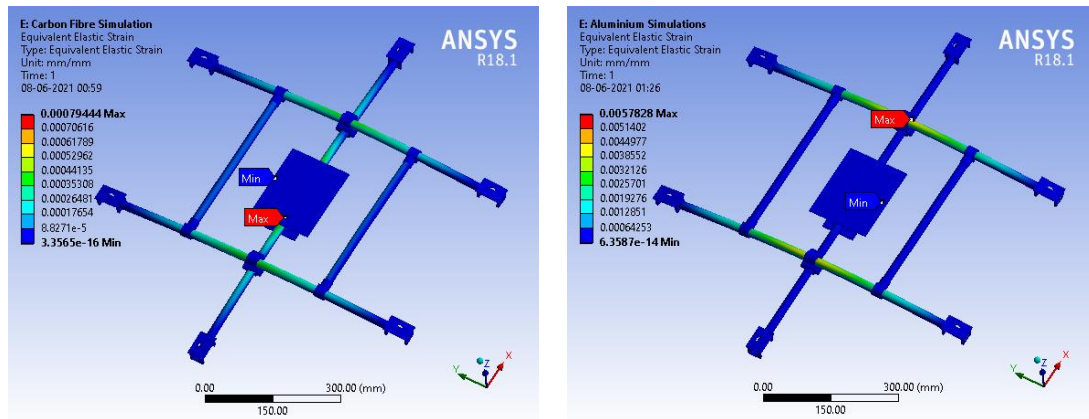


Figure 4.5: Strain Analysis Comparison: a) Carbon fibre b) Al 6061

### 4.3.4 Frame Deformation analysis

For carbon fibre material, the maximum deformation value obtained is **2.18 mm** whereas, for Aluminium 6061, the deformation caused ranges up to **16mm**. Thus, the performance of carbon fibre frame is better compared to Aluminum alloy frame as deformation of carbon fibre is less compared to Aluminium.

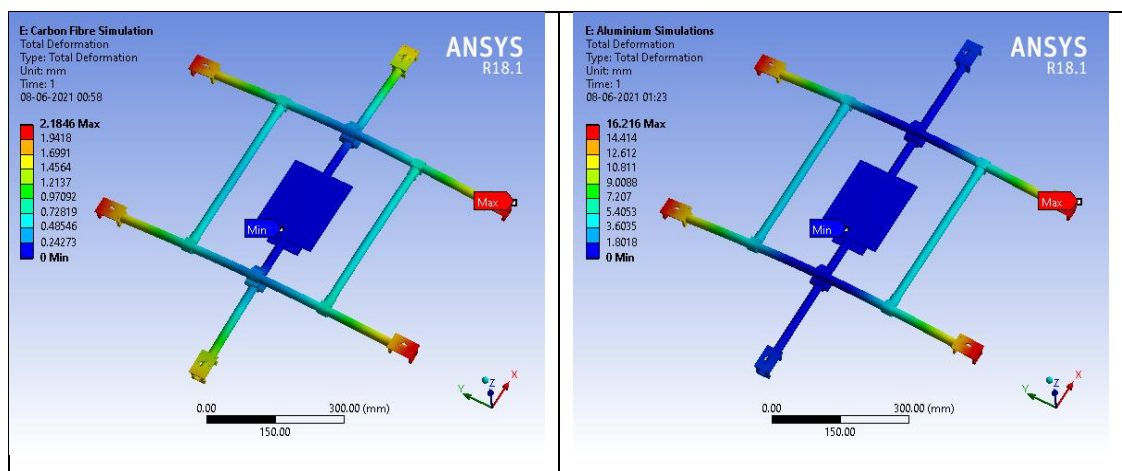


Figure 4.6: Total Deformation Analysis Comparison: a) Carbon fibre b) Al 6061

### 4.3.5 Result

As part of Finite Element analysis, we compared the performance of a carbon fibre frame vis-a-vis an Aluminium frame, employing static structural analysis. From the structural analysis, it was observed, the performance of carbon fibre frame is better compared to Aluminum frame both during stress and deformation analysis. Thus, Carbon fiber offers good stiffness and strength at low density– which is lighter than Aluminium. Lastly taking into account the machining effort, carbon fibre is the preferred choice for Hexacopter frame modelling.

## 4.4 Modal Analysis: CFRP Frame

Based on static structural analysis, we have selected CFRP as our preferred material for the hexacopter frame assembly. We shall now be carrying out the modal analysis of the CFRP frame to determine its natural frequencies and their respective deformations to have a better understanding of our design implications.

### 4.4.1 Modal Analysis: Theory

All structures have natural frequencies. Modal analysis helps us to determine the natural frequencies of the components of a structure that cause resonance. Resonance causes unwanted noise and mechanical stress, strain in the structure leading to premature fatigue /failure. Analysis of these natural frequencies (modes) with Ansys modal Analysis helps us to identify various deformation patterns (modal shapes) like bending/torsion at these frequencies.

The dynamic response of the drone to wind and motor vibrations will be a combination of these natural frequencies with varying amounts of contribution from each of these modes.

### Equations governing Modal Analysis

The governing equation of motion for an n-DOF linear mechanical system is given by.:

$$M\ddot{x}(t) + C\dot{x}(t) + Kx(t) = f(t), \quad (1)$$

where  $M$ ,  $C$  and  $K$  are  $n \times n$  mass, damping, and stiffness matrices respectively.

$x(t)$ ,  $\dot{x}(t)$ ,  $\ddot{x}(t)$  are the vectors of the generalized displacement, velocity and



acceleration, respectively and  $f(t)$  is the vector of generalized (external forces) acting on the system. The  $n$  dimensional vector variable  $x(t)$  indicates a position of a lumped mass  $M_i$  on the structure, and the  $n$  dimensional vector variable  $f(t)$  describes the externally applied force.

Considering free vibrations without damping, then eq (1) reduces to

$$M\ddot{x}(t) + Kx(t) = 0 \quad (2)$$

Assuming its solution as in the form  $x = e^{i\omega t}$

Substituting  $x$  in eq (2) will give

$$(-\omega^2 M + K) X = 0 \quad (3)$$

Solving  $(-\omega^2 M + K) = 0$  gives the natural frequency and solving for  $X$  gives the eigenvector or mode shapes.

### Modal shapes

Mode-shapes tell us how the structure tends to deform at specific natural frequencies. The mode-shapes tell us which regions would experience high stresses if the deformed shape is similar to the mode shape. This is useful because we generally do not want the joint regions to be the region of high stress as it can reduce the life of the structure.

### Participation factor and effective mass

The mode participation factor tells us which modes would be excited the most. The effective masses tell us which modes have to be included in the given dynamic analysis. Effective mass measures the amount of mass moving in each direction for every mode. A high value indicates that the mode will be excited by excitations in a particular direction.

For a given natural frequency  $f$ ,

Time period  $T = 1/f$

Participation factor for  $i^{\text{th}}$  mode:

$$\gamma_i = \{\Phi_i\}^T [M] \{D\}$$

where  $\Phi_i$  = Eigen vector normalized

$[M]$  = Mass matrix

$\{D\}$  = Vector describing the direction

$$\text{Effective mass} = (\text{Participation factor})^2$$



#### 4.4.2 Modal Analysis using Ansys Workbench

We shall be analysing the natural frequencies and deformations in the drone frame selecting Epoxy Carbon UD (230 GPa) as the choice of material.

##### Pre-processing Settings

The material for the structure is selected as **Epoxy Carbon UD (230 GPa)** in Ansys Mechanical. No boundary conditions are set as these are free vibrations of the structure. Modal Analysis of CFRP frame is done for 20 modes and the results obtained are as under:

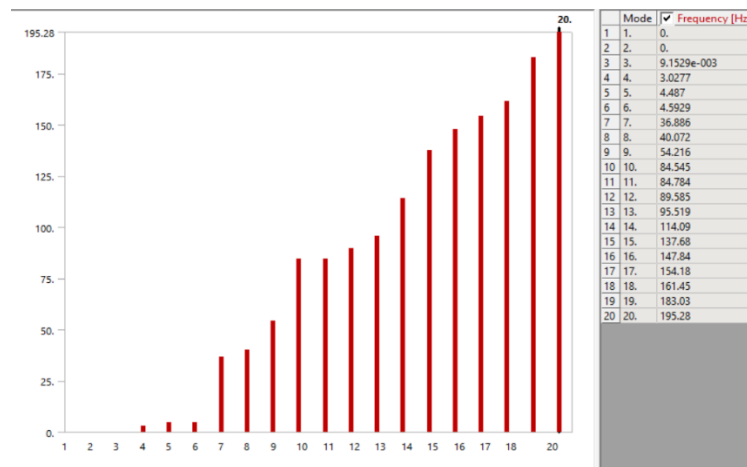


Figure 4.7: Mode vs Natural frequency plot: Carbon fibre Frame

\*\*\*\*\* PARTICIPATION FACTOR CALCULATION \*\*\*\*\*ROTZ DIRECTION

MODE	FREQUENCY	PERIOD	PARTIC.FACTOR	RATIO	EFFECTIVE MASS	CUMULATIVE MASS FRACTION	RATIO EFF.MASS TO TOTAL MASS
1	0.00000	0.0000	-0.29820E-03	0.001341	0.889239E-07	0.178599E-05	0.178599E-05
2	0.00000	0.0000	-0.22754E-03	0.001023	0.517755E-07	0.282587E-05	0.103988E-05
3	0.915289E-02	109.26	0.25131E-03	0.001130	0.631568E-07	0.409434E-05	0.126847E-05
4	3.02769	0.33029	0.18043E-01	0.091128	0.325551E-03	0.654260E-02	0.653850E-02
5	4.48697	0.22287	0.22240	1.000000	0.494626E-01	0.999972	0.993428
6	4.59287	0.21773	0.10668E-02	0.004797	0.113811E-05	0.999995	0.228582E-04
7	36.8860	0.27111E-01	0.17967E-03	0.000808	0.322831E-07	0.999995	0.648387E-06
8	40.0722	0.24955E-01	-0.95400E-07	0.000000	0.910118E-14	0.999995	0.182792E-12
9	54.2164	0.18445E-01	0.56974E-04	0.000256	0.324606E-08	0.999995	0.651953E-07
10	84.5448	0.11828E-01	-0.12893E-05	0.000006	0.166221E-11	0.999995	0.333846E-10
11	84.7839	0.11795E-01	-0.10820E-05	0.000005	0.117078E-11	0.999995	0.235145E-10
12	89.5853	0.11163E-01	-0.45835E-05	0.000021	0.210084E-10	0.999995	0.421943E-09
13	95.5189	0.10469E-01	-0.46441E-03	0.002088	0.215679E-06	1.00000	0.433179E-05
14	114.088	0.87652E-02	0.17777E-05	0.000008	0.316010E-11	1.00000	0.634688E-10
15	137.683	0.72631E-02	-0.53939E-06	0.000002	0.290941E-12	1.00000	0.584338E-11
16	147.841	0.67640E-02	-0.30958E-06	0.000001	0.958401E-13	1.00000	0.192489E-11
17	154.182	0.64858E-02	-0.68074E-05	0.000031	0.463411E-10	1.00000	0.930735E-09
18	161.454	0.61937E-02	-0.65401E-04	0.000294	0.427728E-08	1.00000	0.859067E-07
19	183.026	0.54637E-02	0.32029E-06	0.000001	0.102587E-12	1.00000	0.206040E-11
20	195.281	0.51208E-02	0.12946E-03	0.000582	0.167591E-07	1.00000	0.336597E-06
sum					0.497898E-01		0.999999

Figure 4.8: Participation factor: Carbon fibre Frame

## Modal Analysis Results

20 modes have been extracted for the Carbon Fibre structure giving 20 natural frequencies from 0 to 290 Hz as shown in Figure We could have extracted more modes but they are insignificant. It can be seen from Table that the ratio of effective to total mass is 0.999999 (approaching 1) which implies that we have extracted all the significant modes in the table above.

The participation factor and the effective mass are calculated in the z direction for all these 20 modes. It can be seen from the table that for mode 5 at 4.48697 Hz, contribution in participation factor and effective mass is most significant. All significant vibration mode orders and their corresponding frequencies are listed as under:

Table 4.3: Significant vibration mode orders for CFRP frame

Modal Order	4	5	6	7	9	13	18	20
Frequency (in Hz)	3.0277	4.487	4.5929	36.886	54.216	95.519	161.45	195.28

**Modal shapes.** We have obtained the various deformation patterns (mode shapes) like bending/swinging/torsion at these frequencies. The figure below shows the deformations of the body contour at different locations of the frame for all the eight significant modes. It was observed in Ansys that the vibration modes of modes 4, 5, 6 and 7 are predominantly swinging vibrations while the higher significant modes represent torsional vibrations in the frame body.

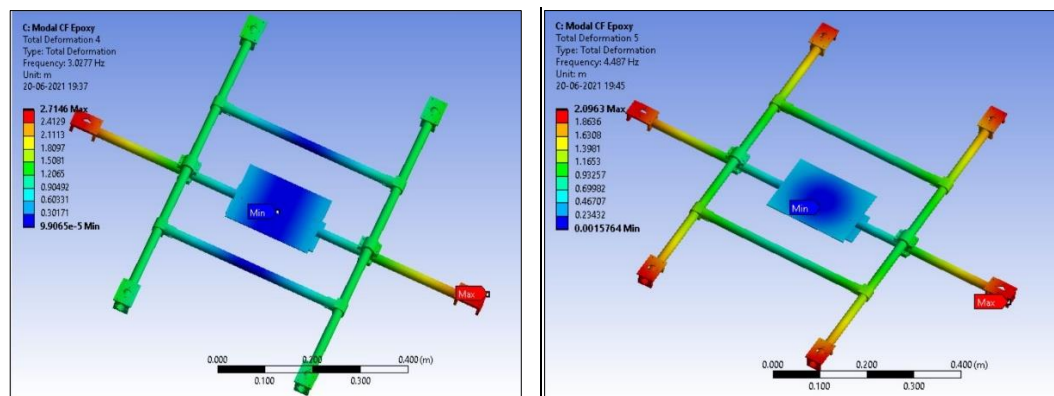


Figure 4.9: CFRP Modal analysis: Mode 4 and 5

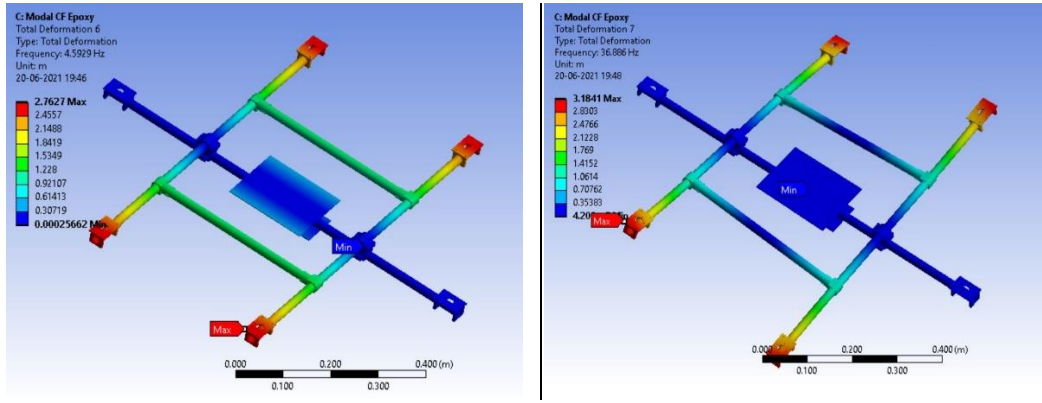


Figure 4.10: CF Modal analysis: Mode 6 and 7

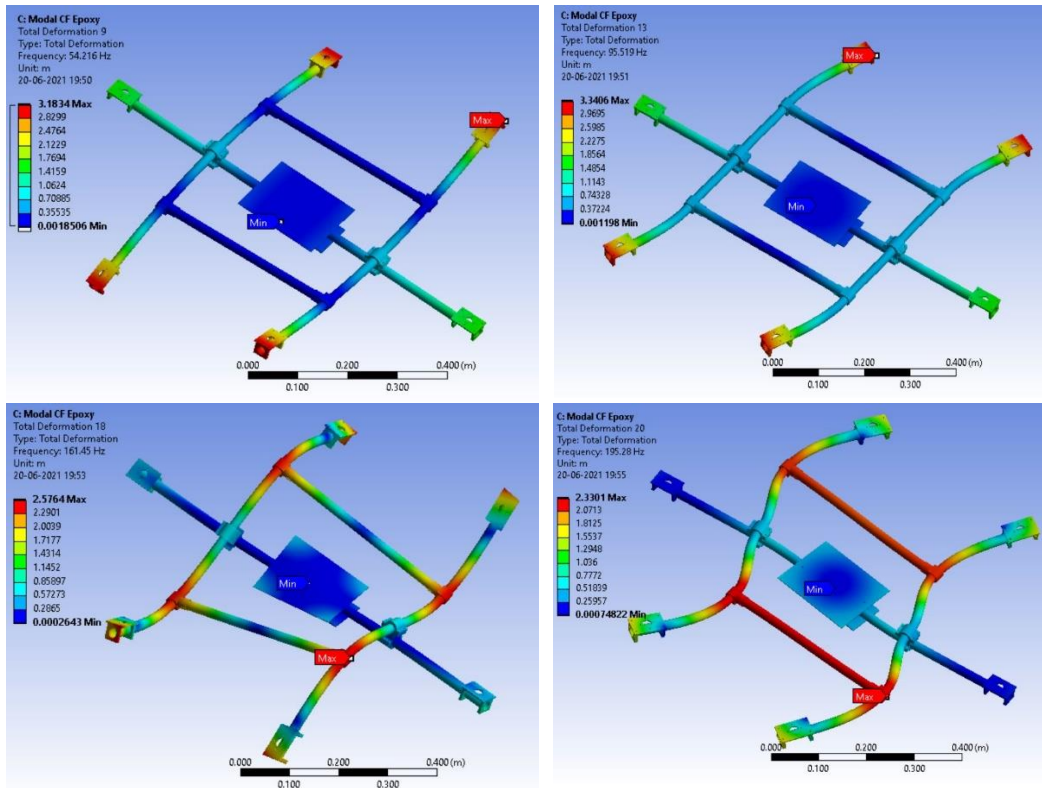


Figure 4.11: CF Modal analysis: Mode 9, 13, 18 and 20

#### 4.4.3 Inference

The main vibration sources during normal operation of the multicopter are the different motor-propeller units. By identifying the natural frequency and modal shape of the hexacopter frame obtained by modal analysis, the possibility of resonance along with associated deformation and failure parts of the drone frame can be predicted. This also necessitates the emphasis to be laid on vibrational damping.

## 4.5 Study of Carbon fibre Frame performance with varying motor thrust

### 4.5.1 Motor Thrust Simulation

Based on load capability and cost inputs, the motor selected was T-motor Antigravity MN4006 KV380 with 15-inch propellers. In this study, structural analysis is carried out on the Hexacopter frame under various conditions when the applied motor thrust is varied from 10 N up to 30 N for different throttle values. As part of loading and boundary conditions, the Hexacopter frame is considered as the load and the centre plate is fixed. Meshing resolution used is fine to get accurate results.

Table. 4.4: Motor Power rating: T Motor MN4006 KV380

T Motor MN4006 KV380 rating for 15-inch propeller							
Throttle	Current (A)	Power (W)	Thrust		RPM	Efficiency	Torque
			gms	N			
50%	3.1	74.40	805	8	3746	10.82	0.152
60%	4.8	115.20	1093	11	4358	9.49	0.203
75%	8.3	199.20	1561	15	5215	7.84	0.285
85%	10.7	256.80	1823	18	5627	7.10	0.334
100%	15	360	2228	22	6177	6.19	0.404

(a) At 60% Throttle when applied thrust at each CF Motor plate = 10 N

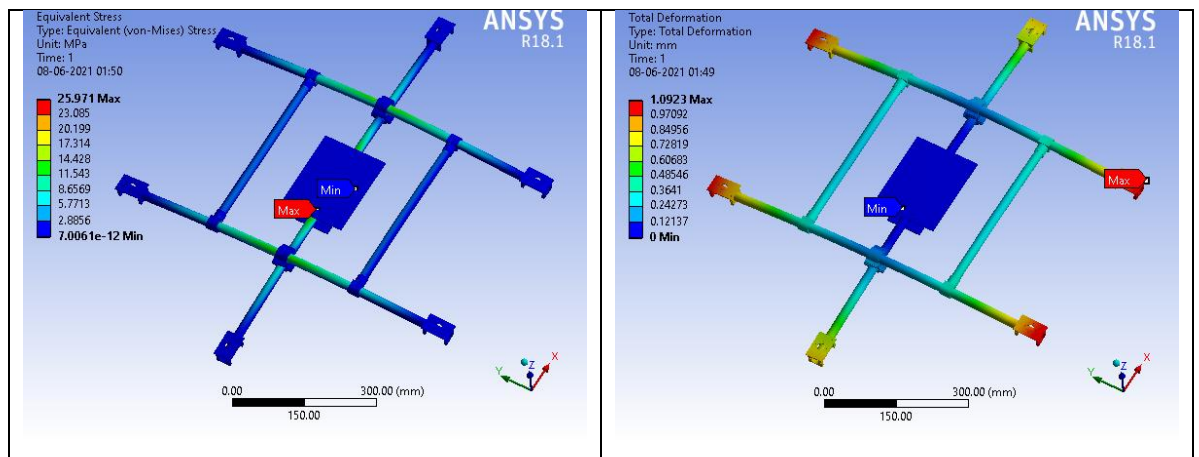


Figure 4.12: CFRP Frame at 10N: a) Stress analysis b) Deformation analysis

**(b) At 90% Throttle When Applied Thrust at each CF Motor plate = 20 N**

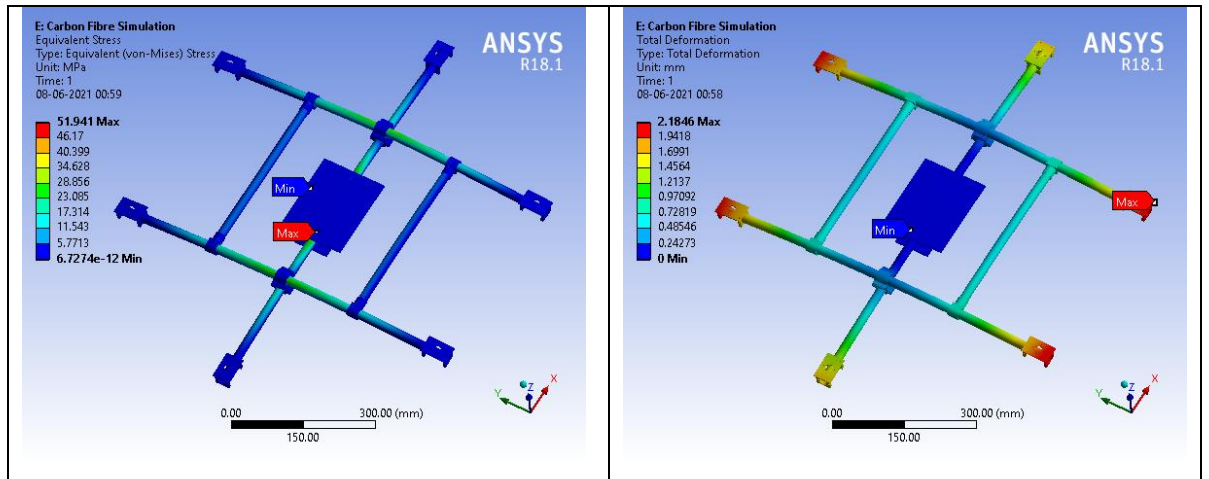


Figure 4.13: CFRP Frame at 20N: a) Stress analysis b) Deformation analysis

**(c) Motor Upgrade case: When Applied Thrust at each CF Motor plate = 30 N**

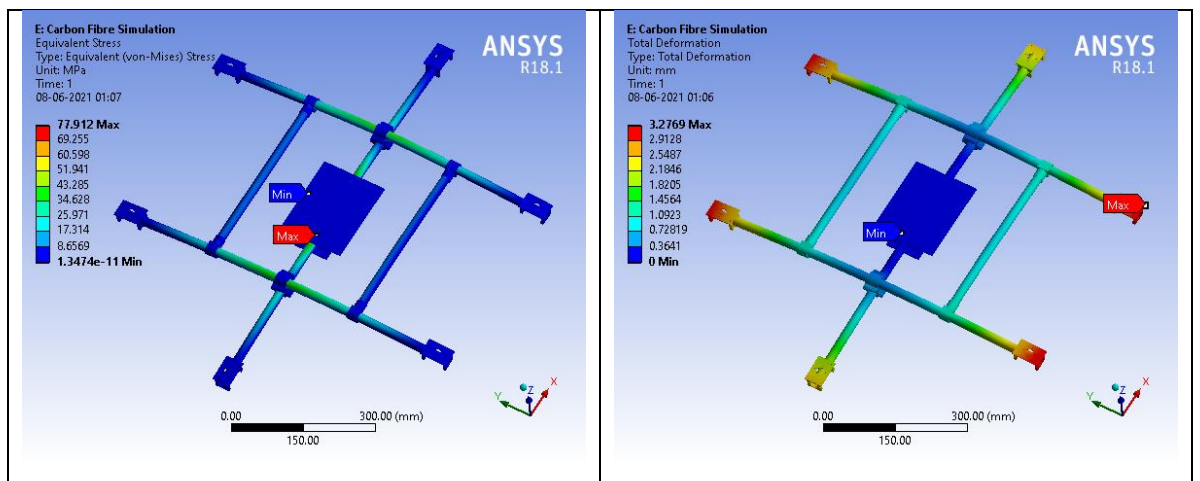


Figure 4.14: CFRP Frame at 30N: a) Stress analysis b) Deformation analysis

## 4.5.2 Simulation Results

As shown in figures, the maximum stress is seen at the outer edge of the arms of the frame shown by red coloured shades. Minimum stress of zero value is obtained at the centre plate of the frame of the hexacopter.

The ultimate tensile strength of CFRP is 290 MPa. For 20N thrust i.e motors working at 90% efficiency, the maximum equivalent stress that is obtained is 51.94 MPa. Hence the frame is safe to withstand the stress generated by the existing selected motors. It can also safely go for a motor upgrade and can take higher thrust up to 3kg force per motor i.e higher payload capability.



# CHAPTER 5

## HEXACOPTER ASSEMBLY

### 5.1 Introduction

There are different steps involved in hardware integration.

- Assembling of Frame
- Wiring and Power supply Connections
- Soldering and Connection of ESCs and BLDC motors
- Assembly of Flight controller and companion computer
- Soldering and integration of Sensors
- Synchronization of Transmitter and Receiver
- Testing of Hexacopter.

### 5.2 Frame assembly

We have identified carbon fibre as the preferred material over Aluminium for the frame based on the FEA analysis results. Frame assembly was carried out using prefabricated 20mm diameter CFRP pipes for drone arms whereas 1 mm thickness plates were used for motor plates and centre plate. Post assembly the weight of the CFRP frame is approx 1.49 kg.



Figure 5.1: Frame Prototype assembly at NCCRD lab, IIT

## 5.3 Motors

Brushless DC motors (BLDC) motors are used for multicopters, as they provide more torque and need lesser maintenance than brushed motors. There are two types of BLDCs- In-runner (inner rotor/ outer stator) and Outrunner (outer rotor/ inner stator). In-runners rotate faster as compared to out-runners while the out-runners provide more torque making them ideal for multicopters.

*Maximum RPM of a motor = Motor KV rating x Maximum battery voltage.*

Usually, for large propellers, motors with low KV ratings and for small propellers with high KV ratings are selected.

Figure 5.2 a) shows T-motor MN4006 380KV motors selected for 1555 propellers to obtain the desired thrust and the table below lists the specifications of the motor.

Max rpm =  $380\text{k/V} \times 24\text{ V} = 9120\text{rpm}$

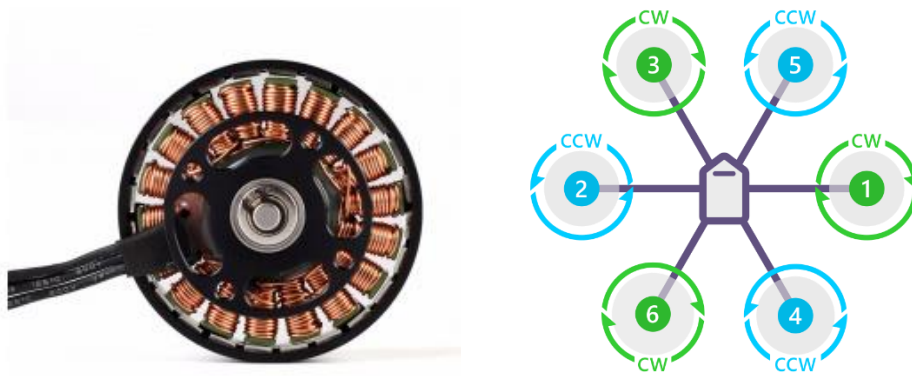


Figure 5.2: a) BLDC motor b) Hexacopter-X configuration

Table 1: Motor specifications: T Motor MN4006 KV380

Motor Specifications			
Internal Resistance	194mΩ	Configuration	18N24P
No of cells (Lipo)	4-6S	Idle current@10V	0.3A
Max Power 180s	380W	Max current 180s	16A
Weight incl cables	68g	Motor Dimensions	35x21mm Dia-44mm
Stator Diameter	40mm	Stator Height	6mm

## 5.4 Electronic Speed Controllers (ESCs)

ESCs control the speed of BLDC motors according to the signals from the controller for maneuvering and hovering. ESCs are selected based on the maximum current drawn by the motors. It can be seen from the motor specifications, that each motor can draw a maximum of 16 amperes of current while producing a maximum thrust of 2.2kg. Also, the existing drone motors would be operated below 85% efficiency. Thus, considering these factors 30A ESCs are selected to control the motors.



Figure 5.3: ESC with rating 5V 30A

## 5.5 Propellers/Rotors

Propellers are selected based on the amount of thrust they can produce depending on motor RPM to obtain the desired performance and altitude of the vehicle. Each propeller should at least provide thrust force equals to the quarter of the weight of the vehicle while rotating within the RPM range of the motor to perform hovering. A propeller is specified by its diameter - end-to-end length and secondly by its pitch - distance covered in one rotation, usually given in inches. The higher the pitch value, the faster the drone goes. Six 1555 Tarot folding propellers (CW/CCW) TL100D04 were utilized for this project to provide the required thrust. Specifications: Diameter 15 inches and Pitch- 5.5 inches.



Figure 5.4: Foldable 1555 propeller pair- CW and CCW



## 5.6 Battery

Batteries have a significant effect on the flight of a drone, such as flight time, speed, and thrust. However, it is always important to use recommended batteries for the selected motors, as higher rating batteries can cause overheating/damaging the motors. A battery is chosen based on the maximum current, the drone can draw at a high discharge rate with reasonable weight for a long and smooth flight. A six-cell LiPo battery is selected which provides 24.1 V with a continuous discharge rate of 16 amps and thus provides the required amount of power to the hexacopter. The in-house developed smart battery with rating 24 V 43Ah was designed for heavy lift drones and needs further optimisation.



Figure 5.5: Six Cells LiPo Battery

## 5.7 Flight Controller

A flight controller (FC) is the most important component of the drone, it is considered as the brain of the vehicle. A flight controller receives data from sensors, analyses the data, and controls the behaviour of the vehicle while performing different maneuvers. We have used the TI Beagle Bone Blue computer which is a fully open-source and Linux-enabled flight controller in this project. The flight controller runs the ArduPilot firmware, which is an open-source, unmanned vehicle Autopilot Software System, capable of controlling autonomous drones, planes etc.

The Beagle board contains the following sensors already inbuilt which are an essential part of flight:

- MPU9250 for accelerometer, gyroscope, and internal compass (I2C)
- BMP280 barometer

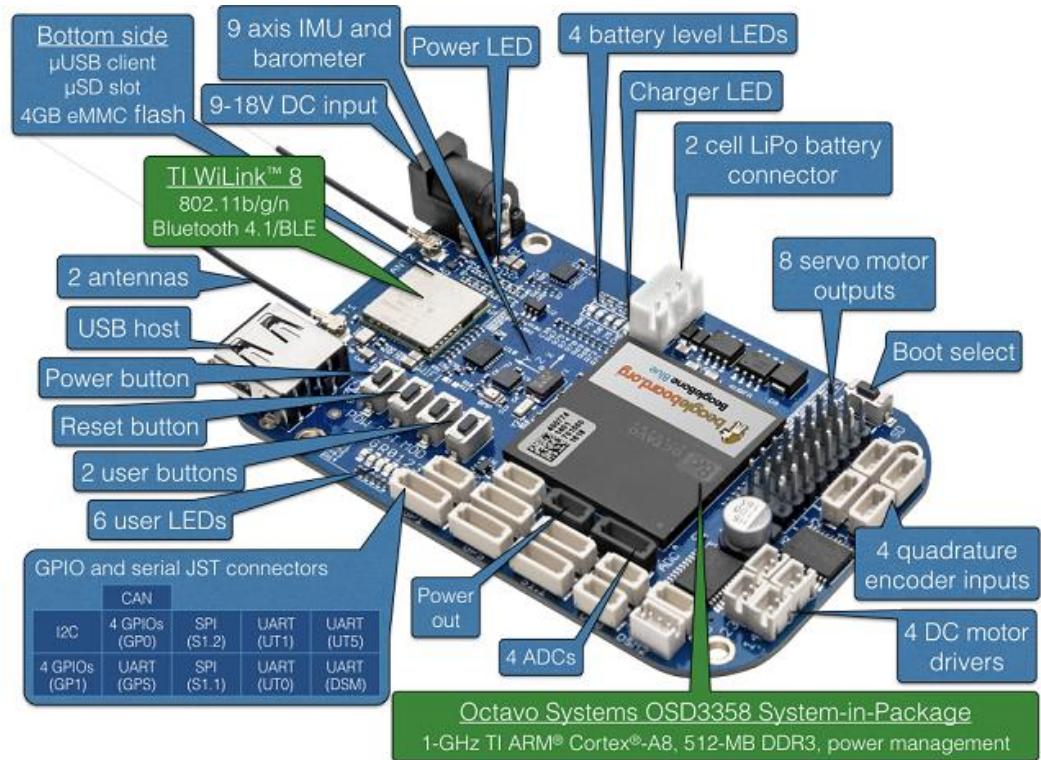


Figure 5.6: Flight Controller

## 5.8 Companion computer

The FC is purely responsible for flight control, and should not be burdened with other signal processing/computational tasks which may then lead to catastrophic failure. For this reason, a companion computer is integrated to perform other computational tasks and pass only a navigation decision to FC.

The companion computer installed on the vehicle communicates with the flight controller, gets all the MAVLink data produced by the autopilot (including GPS data), and uses it to make decisions during flight. It can process live vision feed from an onboard camera or another onboard data source (radar, lidar) for any real-time navigational correction or decision making by the FC. Thus, it enables to perform obstacle avoidance, visual navigation by providing timely processed input to the FC. The drone has a Jetson Nano working as a companion computer, integrated with the FC. It is a small, powerful computer designed to support multiple applications in parallel.



Figure 5.7: Companion Computer

## 5.9 GPS Module

Drones typically orient themselves using GPS, which helps keep them stable while in flight. Drones can carry out waypoint navigation, position-hold, and in case of failure- able to perform RTL ie Return to Launch because of GPS guidance. We have used **GPS Module Ublox NEO-7M** in our system.

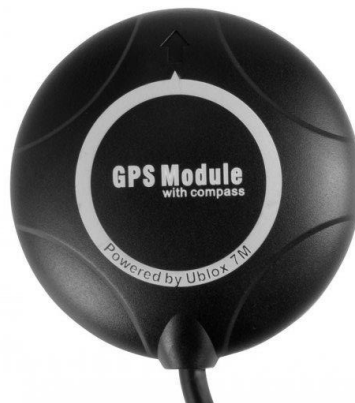


Figure 5.8: GPS Module

## 5.10 Collision Avoidance system

A collision avoidance system, also known as collision warning system, collision mitigation system, or pre-crash system aims to reduce or prevent collision accidents. The system uses sensors or radars to detect any potential obstacle and

send warnings to the pilot of a likely collision based on which he can choose necessary action. Autonomous drones can detect and avoid obstacles by themselves without human intervention. Two different collision avoidance sensors have been integrated on the hexacopter:

### 5.10.1 Lidar

Lidar employs the use of laser beams to calculate the distance of objects around and also create clear images of nearby features. The use of laser beams in the Lidar sensor gives it an edge over the conventional radar, as laser beams are less interfered with as compared to radio waves. Its operation is similar to the IR sensor. A beam is sent out by an emitter which will travel through the air and in case of an obstacle, it is reflected and measured by a receiver. This information is helpful to determine the exact position of the obstacle in reference to the drone's position.

The hexacopter is running with RP A2 360 Lidar. It is a 360-degree 2D laser scanner (LIDAR) that can take up to 4000 samples of laser ranging per second with high rotation speed.

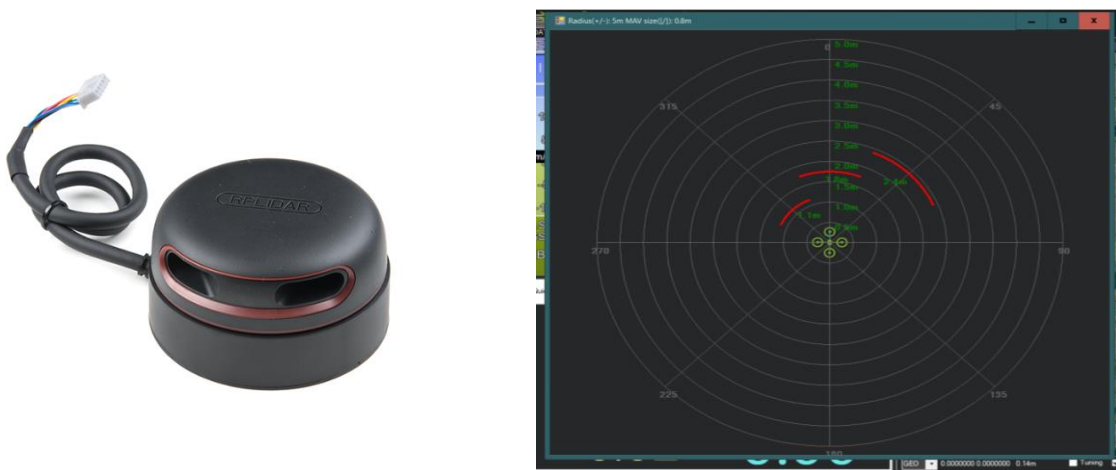


Figure 5.9: a) RP A2 360 Lidar b) Lidar Output

### 5.10.2 Millimeter-wave Radar

Radar systems transmit electromagnetic wave signals to determine the range, velocity, and angle of the obstacles in their path, by capturing the reflected radio signals from

the object. We have integrated mmWave radar from Texas Instruments (TI) IWR6843 Antenna on Package (AoP) as a proximity sensor for obstacle detection and collision avoidance. It operates in an mm-wave band from 60-GHz to 64-GHz band and uses FMCW radar technology for detection and ranging.

## 5.11 Camera with gimbal

Drone gimbals keep a camera in the same position regardless of the motion of the drone. A gimbal is designed to keep the camera at the same angle regardless of the movement of the drone by automatically compensating using calibrated and often remotely controlled electric motors. A camera has been mounted for surveillance capability and further object identification is being done at the ground station terminal using AI-enabled software *Yolo*. We have mounted an Amigo HD camera on a Tarot make gimbal on the hexacopter.



Figure 5.10 a) HD camera b) Gimbal 3D

## 5.12 Radio transmitter and receiver

The radio receiver is connected to the flight controller board of the Hexacopter. The function of the receiver is to send the RC signal to the controller according to the stick movements of the radio control transmitter by which the motion of a drone can be controlled. FrSky Taranis Q X7 Access Transmitter which supports up to 16-channels at 2.4 GHz frequency is paired with the onboard receiver FrSky X8R 16ch Receiver.

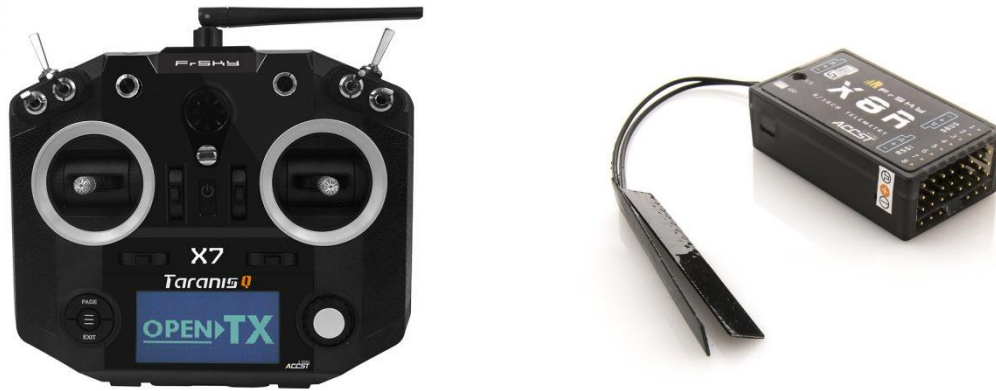


Figure 5.11: a) RC Transmitter b) RC receiver

## 5.13 Final Prototype

The final assembly involved a detailed process of planning the power distribution and space management for mounting the flight controller and Companion computer and positioning various sensors to avoid interference.

### 5.13.1 Layout

A 3-tier arrangement has been done at the centre of the hexacopter for ease of access for repairs and to maintain the centre of gravity. The 24V battery pack has been mounted on the Battery support plate underneath the central CFRP plate. The power components i.e all the power distribution boards, DC-DC converters have been assembled on the central CFRP support plate. On top of this plate, an acrylic board has been mounted which houses the flight controller and the companion computer.

### 5.13.2 Power supply Arrangement

The 24 V power supply is fed directly to the six BLDC motors and is also stepped down to 12 V to be fed to the Beagle Bone Blue controller. The 12 V is further stepped down to 5V using DC-DC converters to power various sensors ie GPS, Lidar, Camera, radio. Though the flight controller is capable of powering the sensors but to avoid any damage, power distribution to all the sensors has been separated from the Flight controller and has been given separately from the 5V DC supply.



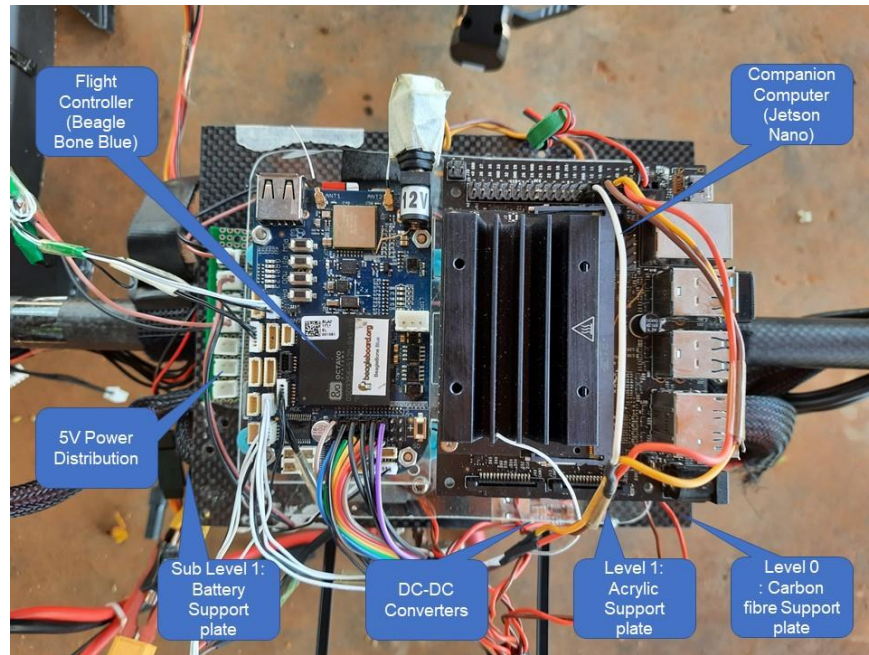


Figure 5.12: Assembly of Flight controller System

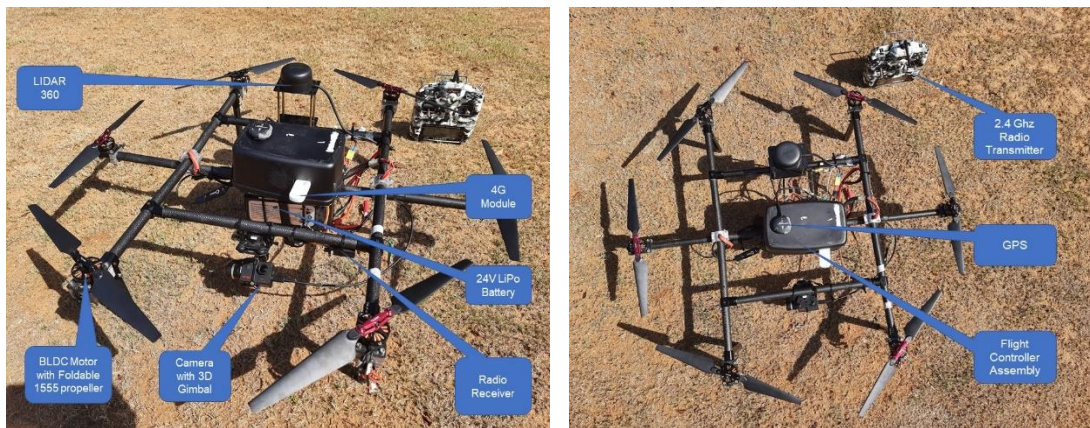


Figure 5.13: Final Prototype a) Front View b) Top view

### 5.13.3 Weight Calculation

Table 5.2: Hexacopter Weight Calculations

Srl No	Components	Weight(gm)
1.	CFRP Frame	1490
2.	Flight Controller	36
3.	Companion computer	249
4.	BLDC motors (6 nos)	408
5.	Electronic speed Controller (ESC) (6 Nos)	327

6.	Propeller (1555)	396
7.	Li-Po battery 16000mAh	1900
8.	GPS module	26
9.	RPLidar A2 360 degree	190
10.	mmWave Radar	20
11.	Camera	110
12.	3D Gimbal	160
13.	Miscellaneous	180
	<b>Total weight</b>	<b>5492gm</b>

Hence the total weight of the hexacopter is 5,492 grams. Now taking Thrust to Weight Ratio (TWR) as 2, the required thrust from each motor is determined as follows:

Thrust = Total weight x TWR

Thrust =  $5492 \times 2 = 10984$  grams

number of motors = 6

Required Thrust per motor =  $1831$  grams =  $18$  N

Thus, for the ability to fly and hover, the heavy-lift hexacopter must overcome the gravity force. Based on the above calculation, each motor must produce a thrust of 18N with the assumption that all motors have equal thrust. To ensure the thrust of the rotor that is used is capable of lifting and moving the hexacopter, it is necessary to measure the thrust of the rotor.

## 5.14 Flight Testing

Table 5.3: Test Flight Results of Hexacopter

Srl. No.	Design Criterion	Design Parameter	Test Flight Results
1.	Payload capacity	Up to 1 kg	A maximum of 0.8 kgs was tested
2.	Flight endurance	Up to 15 mins	15 mins for 0.8 kgs payload
3.	Fly options	Manual, GPS aided, Autonomous	All tested successfully



4.	Fly height	Up to 500 ms	Tested up to 50 m due to Flight Zone restrictions
5.	Fly range	Up to 2 Km	Tested up to 0.8 km with a clear line of sight



Figure 5.14: Test flight in progress at Chemplast Cricket Stadium



Figure 5.15: Ground Control station setup

## 5.15 Challenges faced and addressed:

- **EKF Variance.** Lidar 360 rotations caused higher vibrations on the frame. This caused EKF variance errors in autopilot. The Lidar was re-sited away from the FC assembly, onto the arms. Further measures were taken to dampen these vibrations.
- **Enclosure for Circuitry.** Dust and moisture proofing of FC assembly was essential to avoid damage to the onboard circuitry. An enclosure was modelled but could not be 3D printed due to printer unavailability. So, an ABS plastic box was re-appropriated as an enclosure. Heat sinks were placed for heat dissipation.
- **Centre of gravity.** The position of the battery and flight controller was rearranged in initial design iterations to maintain the CG of the drone. The same was also ensured when lidar and camera with gimbal were mounted on the drone.
- **Troubleshooting.** Assembly of all power components, wiring, and FC on the same CF plate created clutter and affected troubleshooting. The separation of power supply components and other components was done into two tiers. Wire color coding further eased the diagnosis process.
- **Delays.** Pandemic scenario reduced the available time for trials and testing and also affected procurement of components due to delays in shipments.

## CHAPTER 6

### FLIGHT DATA ANALYSIS

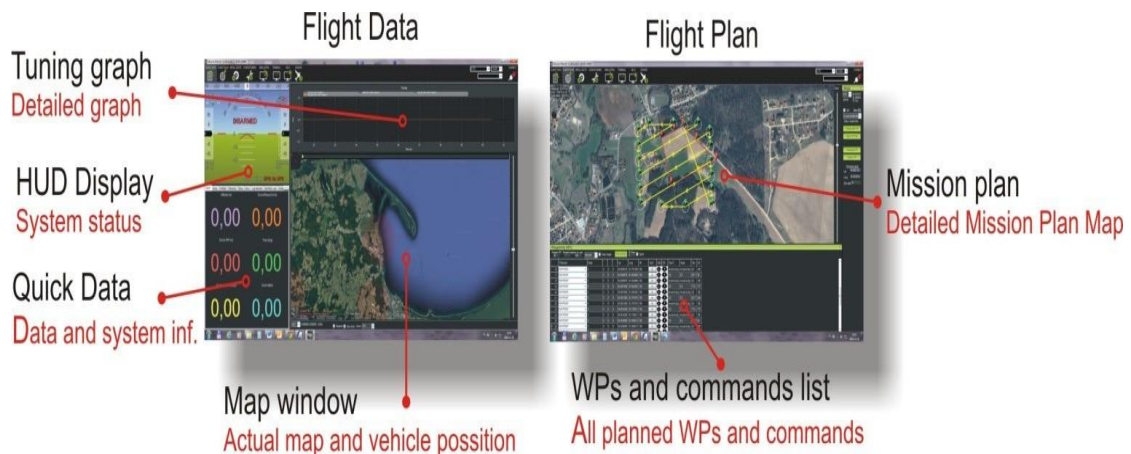
#### 6.1 Introduction

Mission Planner is a Ground controller Station (GCS) software application that communicates with the open-source autopilot firmware ie ArduPilot residing on the flight controller using Micro Air Vehicle Link (MAVlink) protocol. The purpose of Mission Planner is to connect to the autopilot to receive telemetry data and control the vehicle. The basic GCS configuration consists of a Windows PC with installed Mission Planner Software or an Android phone running the same. Linux users are provided with APM Planner 2 software. The GCS communication channels can be established via Internet/radio/ WiFi/ Bluetooth, all using MAVLink protocol.

#### Features

Mission Planner supports:

- updating the automatic pilot firmware (Figure 10a);
- live reading of telemetry data and reading offline sensor data (Figure 10b); setting up and adjusting the autopilot system and planning a flight mission;
- connecting with a flight simulator;
- downloading log files and analyzing them



## 6.2 Mission Planner Setup

Once the drone is connected to Mission planner on MAVlink basic configuration of FC is done as per the type of drone selected- *Hexacopter X frame type*. Then calibration of the compass, accelerometer of the drone is done with the Mission planner. Further calibration of radio, ESCs, motors, tuning, and adjusting PID loops is done to configure and tune the flight controller so that the pilot can properly control the UAV from the ground.



Figure 6.2: Mission Planner: a) Firmware selection b) Drone Calibration

## 6.3 Flight Data Log

Flight log data provides information about various operating parameters such as UAV (pitch, yaw, roll) and velocity data on the three axes; data about GPS parameters (position, speed, altitude, compass head), mission type data; data on navigation and servo output signals; data about radio signals.

Flight data logs can be used to analyse and diagnose mechanical defects, vibrations, magnetic interference, or engine operation, these flaws occurring in the form of pitch, roll, or girth leaps. Vibrations with significant values can be read by displaying data provided by accelerometers of IMU messages for horizontal position control. Magnetic interferences that may be generated by the power distribution board, motors, accumulators, ESCs can cause malfunction of the compass that causes unwanted UAV behaviour.

There are two types of flight log data recorded about the flight data which can be analysed:

Table 6.1. Comparison of Log files on Mission Planner

Feature	Types of Logs	
	Data flash log	T Logs
Task	Recorded on Drone Autopilot	Recorded by Ground station
Storage location	SD card	On GCS PC via telemetry link
File Format	.bin	.tlog

## 6.4 Analysis of Flight Data

The drone is capable of flying in several modes. The main modes are manual mode, Loiter mode, and autonomous mode. In manual mode, the drone is controlled by RC and in others modes, the drone flies autonomously. We have conducted more than 15 experimental flights involving the implemented UAVs and all the flight data have been collected. We would analyze specific cases here and analyse the data.

### 6.4.1 Case study 1: Position hold mode

Here we would have analyzed a particular case wherein the hexacopter covered a short flight at the IITM research park in position hold mode.



Figure 6.3: Hexacopter in Position Hold mode



### a) Flight Trajectory

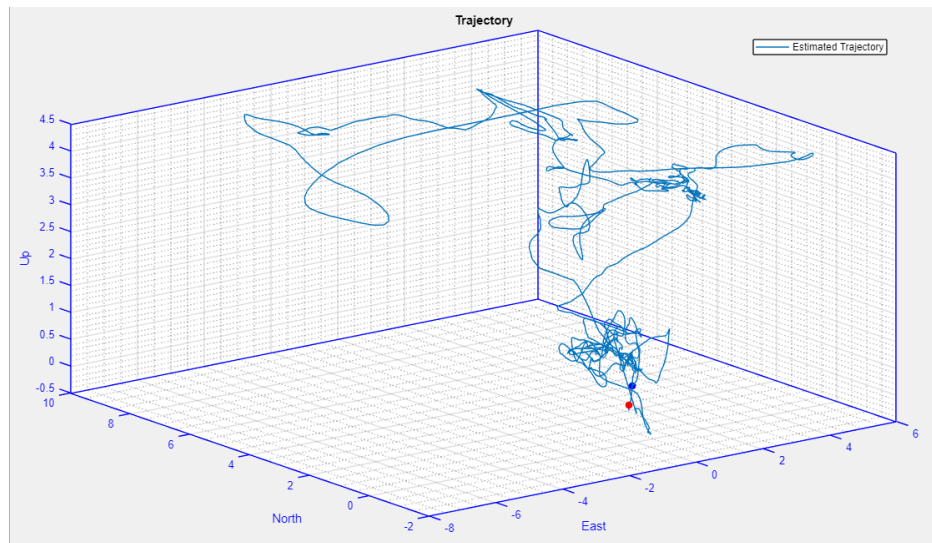


Figure 6.4: Manual Flight Trajectory on Matlab

### b) GPS Fix Analysis

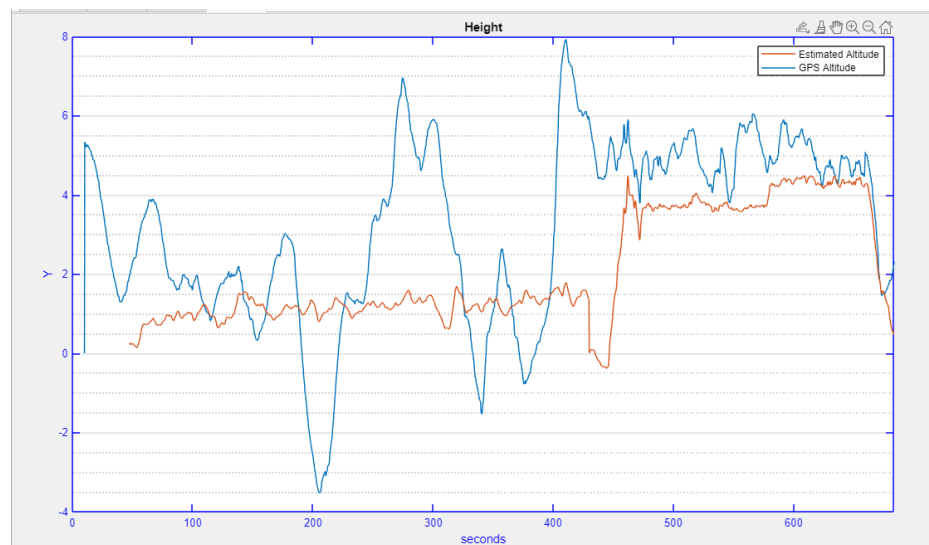


Figure 6.5: Manual Flight Parameters: Altitude & GPS

**Location:** IITM Research Park.

**Flight Duration:** 11.4 Minutes (approx.)

**Altitude:** Max 5m; **Rate of Climb:** 0.79m/sec (Max)

**Observation:** Satellite Visibility - Ranged between 11-13 (value >12 is required) with a mean of 11.85 which indicated varying GPS coverage which affects the Horizontal degree of precision of the drone.

### c) Vibration Analysis

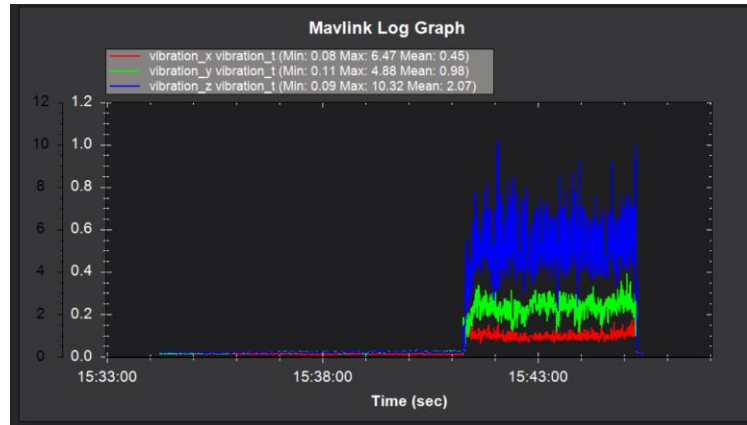


Figure 6.6: Manual Flight parameters: Vibrations along X, Y, Z axes

**Observation:** Initially the vibrations observed were negligible. Spike in vibrations was observed with altitude gain but within permissible limits.

**Analysis:** The graph shows acceptable vibration levels which are consistently below 30m/s/s.

### d) Attitude Performance

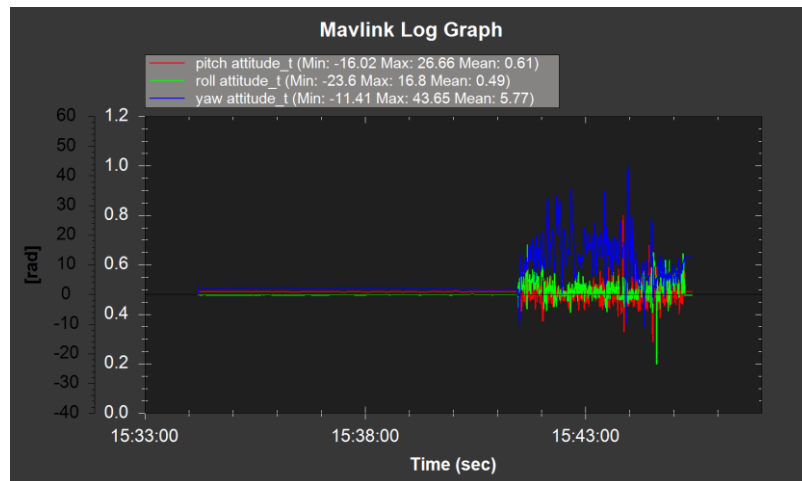


Figure 6.7: Manual Flight parameters: Roll-Pitch-Yaw Performance

The Roll, Pitch, and Yaw performance of the drone can be seen when the drone was put into position hold mode. The attitude performance was stable and no major divergence is seen in the plot.

## 6.4.2 Case study 2: Variances/ Errors

Various errors/variances like compass error, EKF variance, yaw variance, accelerometer error etc were studied/rectified during the course of trials of which two instances are listed as under:

### a) Yaw variance

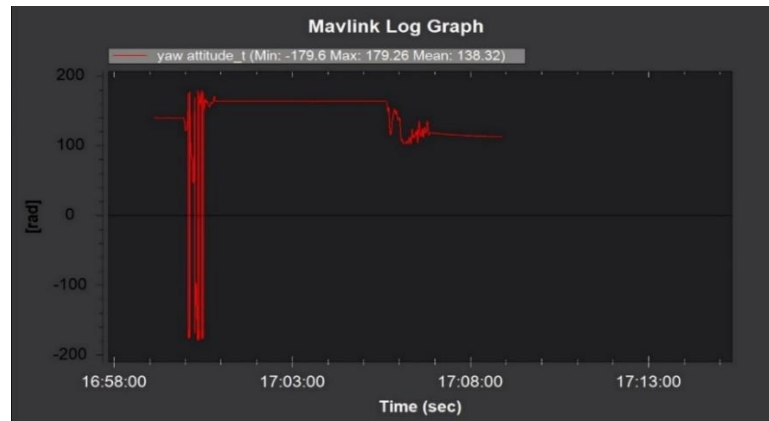


Figure 6.8: Flight parameters: Yaw Variance

The yaw performance was not stable as some major divergence is seen in the plot during position hold mode. One possible reason may be due to imbalance created by a motor plane misalignment or due to improper frame calibration. Thus, it requires yaw tuning.

### b) Throttle Output error

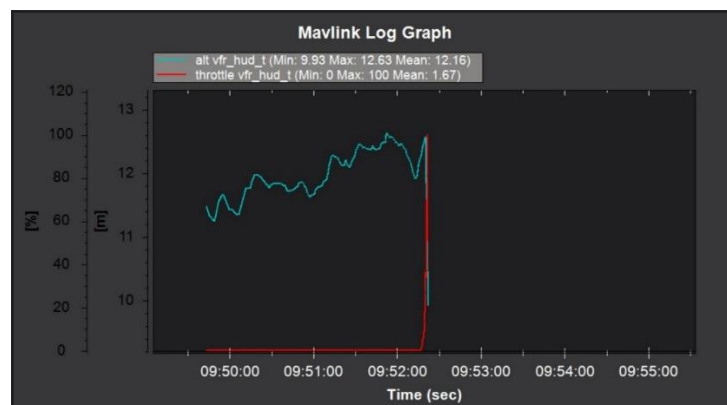


Figure 6.9: Flight parameters: Throttle output error

The plot shows a sudden rise of throttle to its maximum value resulting in the drone rising to 12 metres in a fraction of few seconds. This may be due to improper radio calibration between the RC receiver and drone.



### 6.4.3 Case study 3: Autonomous Mission

Here we would have analyzed a particular case wherein hexacopter covered a short flight from Chemplast cricket stadium to football stadium on an autonomous mission. 4 waypoints were marked along the route. The salient aspects of the flight are as under:

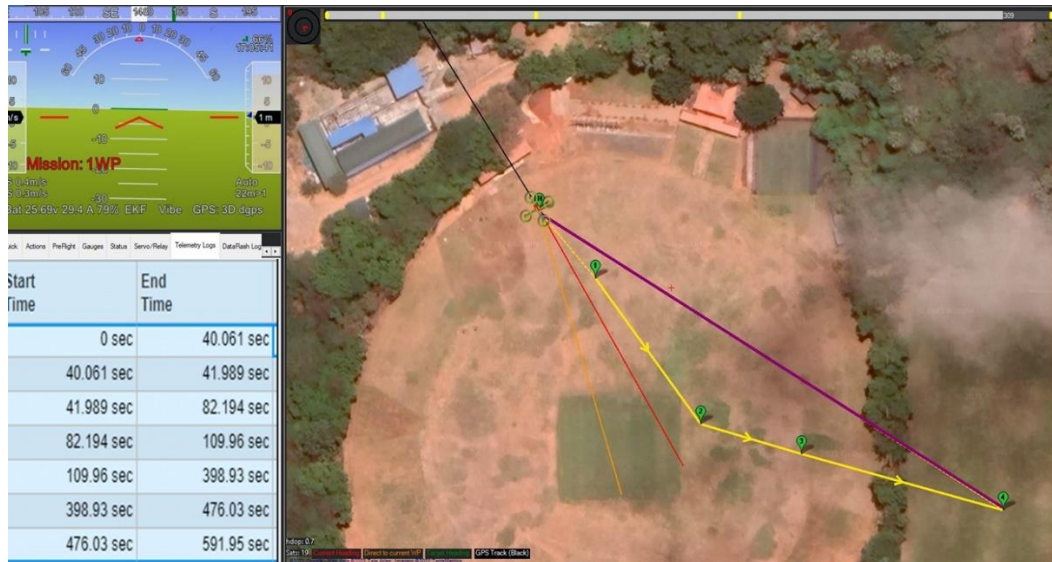


Figure 6.10: Hexacopter Autonomous mission

#### a) Flight Trajectory

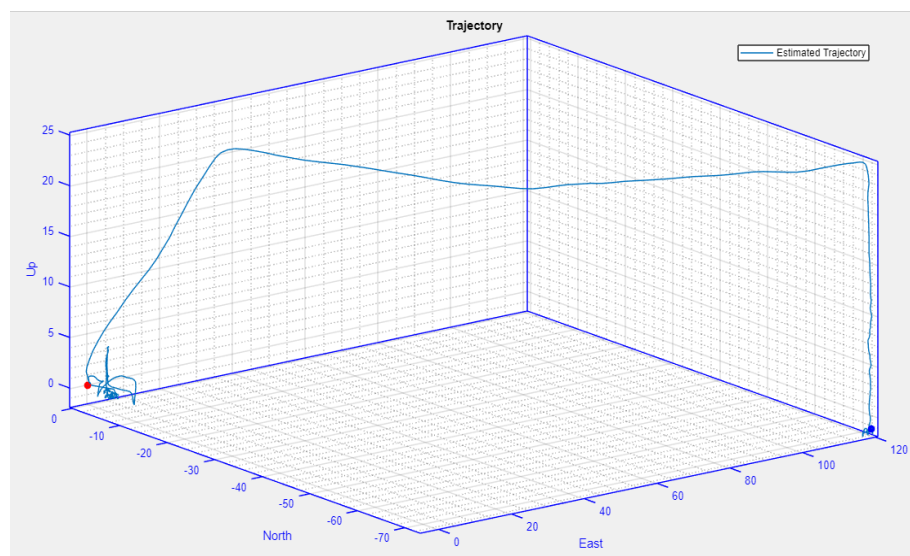


Figure 6.11: Auto Flight Trajectory on Matlab

## b) GPS Fix Analysis

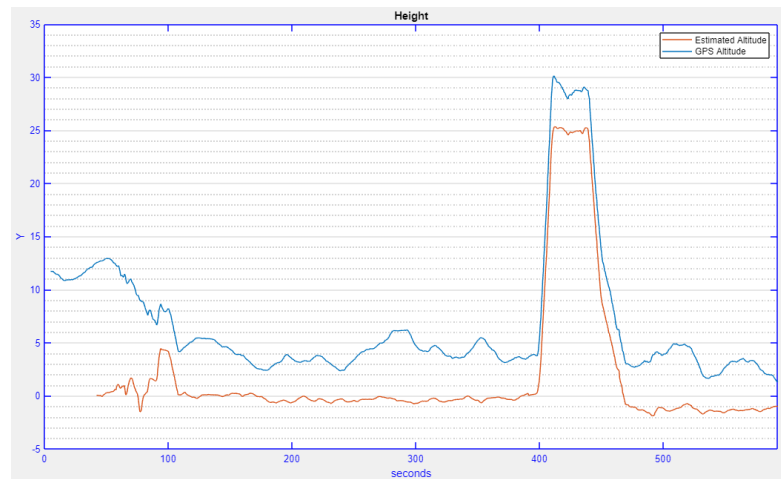


Figure 6.12: Auto Flight Parameters: Altitude & GPS

**Location:** Chemplast Stadium IIT.

**Flight Duration:** 10 Minutes (approx.)

**Observation:** Satellite Visibility - Ranged between 16-20 (value >12 is required) with mean of 18.77 which indicated adequate GPS coverage.

**Altitude:** Max 30.13m; **Rate of Climb:** 5m/sec (Max)

## c) Vibration Analysis

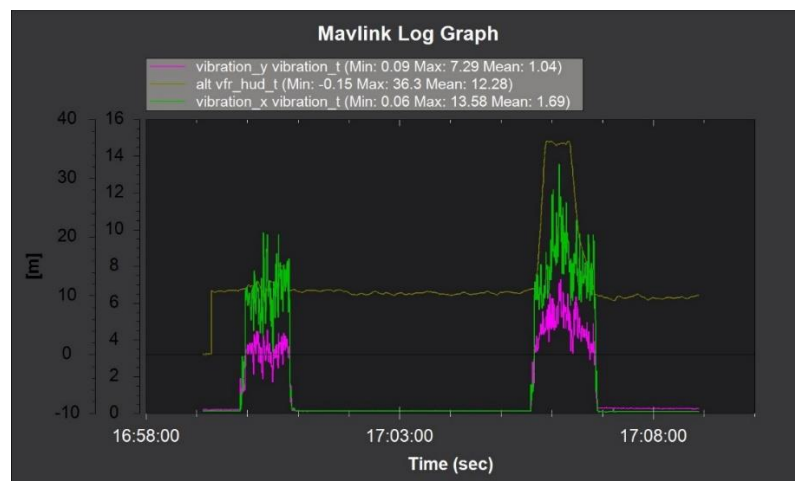


Figure 6.13: Auto Flight parameters: Vibrations along X, Y, Z axes

**Observation:** At an alt of 10m, vibrations observed were negligible. Spike in vibrations were observed with altitude gain, but within permissible limits.

**Analysis:** Vibration values increase with the increase in altitude due to higher motor thrust with position or altitude hold. The graph shows acceptable vibration levels which are consistently below 30m/s/s which indicate the frame is sturdy.

#### d) Voltage Drop vs Time

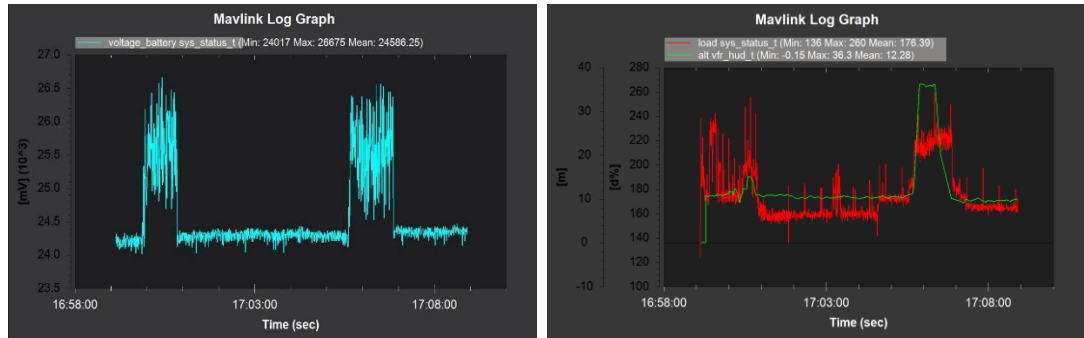


Figure 6.14: Auto Flight parameters: Voltage and Load

It is observed that the Battery voltage was stable initially but varied continuously during the flight between 26 V and 24V due to high power requirements during vertical lift and while maintaining altitude.

#### e) Attitude Performance

The Roll and pitch performance of the drone was stable and no major divergence is seen in the plot.

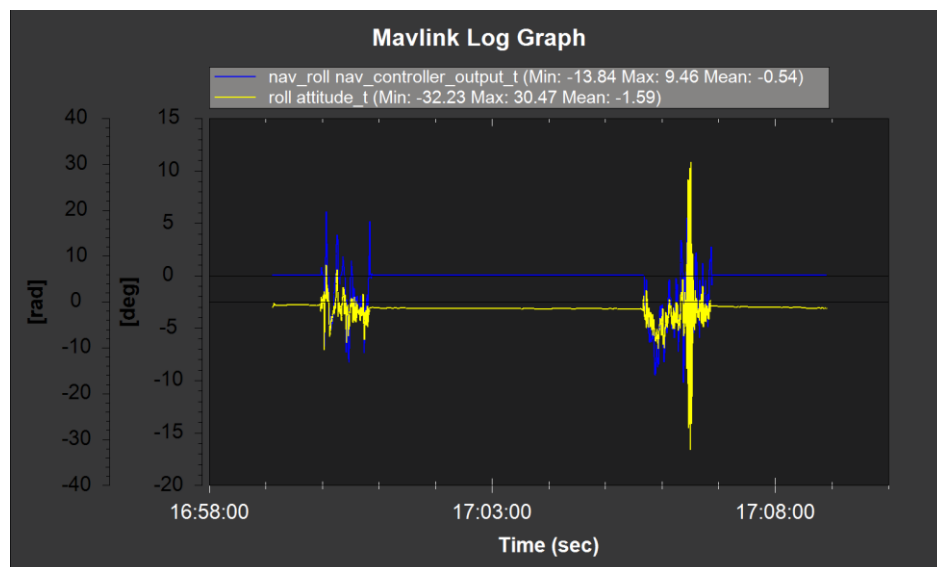


Figure 6.15: Auto Flight parameters: Roll Movement

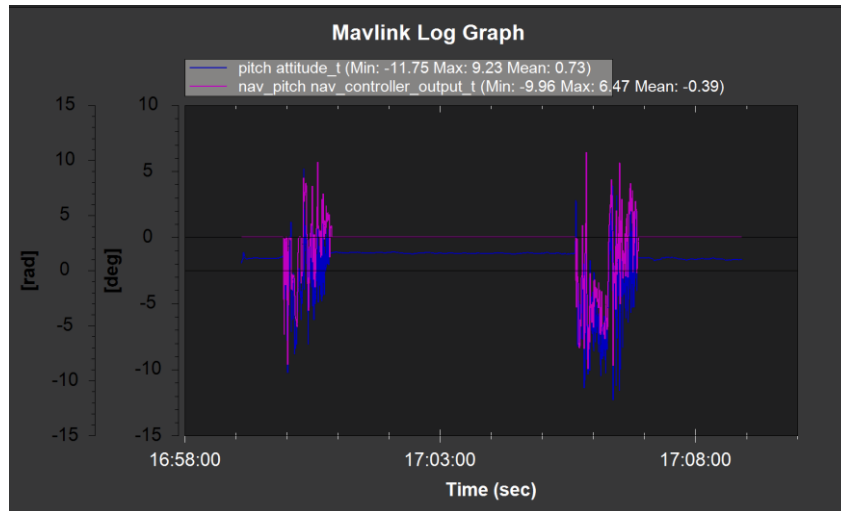


Figure 6.16: Auto Flight parameters: Pitch Movement

## 6.5 Results

The implemented system is capable of flying in different modes. This system has been configured with Mission planner, a powerful ground station that enables the user to view flight data, upload parameters or even override a mission in real-time flight condition when a mission is running. From entire the log analysis, we can conclude that the overall performance of our system i.e movement, orientation, motion is stable.

## CHAPTER 7

### CONCLUSION

In this thesis, we studied the various aspects of building a frame right from frame designing using CAD modelling on Fusion 360, material selection and design simulations using Ansys mechanical. We carried out Modal analysis and Static Structural Analysis over the Frame model to compare Carbon fibre Reinforced Polymer (CFRP) material with Aluminium 6061 alloy. The results have shown that the von mises stress and deformation was lesser in a Carbon fibre frame vis-a-vis an Aluminium 6061 frame. After three design iterations, we finalized our frame design keeping aspects of aerodynamics, structural integrity, CG, and vibrational damping aspects.

Post building the frame, the physical assembly of various components and sensors was done into the frame. Flight log analysis using the Mission Planner application helped us to understand the structural behaviour throughout the flight. It also gave us insight into the performance of the hexacopter and helped in troubleshooting certain issues faced in system integration and also optimizing the design of the final prototype.

#### **Future Work**

The existing drone design can be optimized further by replacing the existing metal joints with Carbon fibre joints and tube connectors. Similarly, the existing motors can be replaced by higher thrust motors as the frame can support the same, as evident in the simulations. The advantage of the existing frame design is that it is scalable to accommodate a higher payload. The same design can be scaled up to support the new motors and smart battery developed in-house.

## References

- [1] Serkan Caskai, Kadir Gok, Mustafa Aydin, Ikbai Ozdemir, 2020. Finite element method based structural analysis of quadcopter UAV chassis produced with 3D printer.
- [2] Saad Fareed, 2019. Vibrational Analysis of Quadcopter Using FEM Technique.
- [3] MD. Faiyaz Ahmed, Mohd. Nayab Zafar, J. C. Mohanta 2020. Modeling and Analysis of Quadcopter F450 Frame.
- [4] D Susitra, E Annie Elisabeth Jebaseeli, Venkata Kishore Chitturi and Vineet Chadavalavada 2020, Design and development of an Hexacopter for fertilizer spraying in agriculture fields.
- [5] Rahul Singh, Rajeev Kumar, Abhishek Mishra, Anshul Agarwal, 2019. Structural Analysis of Quadcopter Frame.
- [6] Paweł Burdziakowski, 2017. Low Cost Hexacopter Autonomous Platform for Testing and Developing Photogrammetry Technologies and Intelligent Navigation Systems.
- [7] V Prisacariu et al 2018 Considerations regarding open-source systems and equipment for UAV's.
- [8] Charaf Bennani Karim, 2020. The design and development of a general-purpose drone.
- [9] Tuton Chandra Mallick, Mohammad Ariful Islam Bhuyan, Mohammed Saifuddin Munna, 2016. Design & Implementation of an UAV (Drone) with Flight Data Record
- [10] J. Verbeke, S. Debruyne, 2016. Vibration analysis of a UAV multicopter frame.
- [11] V. Artale, C.L.R. Milazzo and A. Ricciardello, 2013. Mathematical Modeling of Hexacopter.
- [12] M. Aswath and S. Jeevak Raj 2021. Hexacopter design for carrying payload for warehouse applications.
- [13] V Prisacariu<sup>1</sup>, I Cîrciu<sup>1</sup> and A Luchian, 2016. Considerations regarding open-source systems and equipment for UAV's.
- [14] Akshay Balachandran, Divyesh Karelia, Dr. Jayaramulu Challa, 2014. Material selection for unmanned aerial vehicle.
- [15] Jinbao Chen, Hong Nie, Zemei Zhang, Lichun Li, 2013. Finite element linear static structural analysis and modal analysis for Lunar Lander.

- [16] Zhang Jinguang, Yang Hairu, Chen Guozhi, and Zhang Zeng, 2017. Structure and modal analysis of carbon fiber reinforced polymer raft frame
- [17] M Urdea, 2021. Stress and vibration analysis of a drone.
- [18] Working Principle and Components of Drone, extracted from <https://cfdflowengineering.com>
- [19] DGCA ATL\_Drone\_Module under Atal Innovation Mission from <https://aim.gov.in/>
- [20] Learning resources, extracted from <https://ansys.com>
- [21] Mission Planner documents extracted from <https://ardupilot.org>